國立臺灣大學生命科學學院植物科學研究所

碩士論文

Institute of Plant Biology

College of Life Science

National Taiwan University

Master Thesis

HDA15 互作蛋白之鑑定與分析

Identification and characterization of the interaction proteins of HISTONE DEACETYLASE 15

葉培民

Pei-Ming Yeh

指導教授：吳克強　博士

Advisor: Keqiang Wu, Ph.D.

中華民國 104 年 12 月

December 2015

致謝

在完成碩士學位的兩年多的時間裡，受了許多的幫助在心中有著許多的感謝。首先十分感謝父母，在是否要研讀碩士選擇上給予我充分的空間以及最大的支持，並且在我實驗忙碌很少回家這件事給予很大的寬容與體貼。再者我要感謝吳克強老師讓我加入 R1026 這樣一個資源充足而且團隊氣氛佳的實驗室並將我指派給佳陽學長指導，讓我能順利完成我的碩士論文。很感謝實驗室裡的陳佳陽學長對我的實驗技術指導，願意花費許多時間幫助我修正錯誤並十分耐心地與我討論實驗，面對實驗困境。此外也十分感謝游竣惟學長與杜佾璁學姐在平時對我的實驗上的提醒與討論使我的實驗能順利精確。也感謝實驗室的各位成員，多位學長姐以及學弟妹們，瑞緹、欣憲、盟勝、燊琪、珮仔、華駿與松諺平時在實驗上的協助幫忙。另外特別感謝我的同屆戰友昱豪、莊菱與威廷在實驗不順利的時候給予打氣，在實驗順利時給予肯定與掌聲使我即使在顛頗的實驗道路上仍能順利堅強的向前。謝謝大家這段時間的陪同與照顧，讓我能順利完成我的碩士論文。

摘要

組蛋白去乙醯酶(HDACs 或者 HDAs)主要作用於組蛋白 N 端離氨酸的去乙醯化作用，而此修飾在植物生長發育過程中扮演重要角色。組蛋白去乙醯酶 HDA15 為 RPD3/HDA1 superfamily 的成員，目前已知的功能為與 PIF3 共同調控葉綠素的生合成與光合作用。我們使用 LC-MS/MS 找到了許多可能與 HDA15 有交互作用的蛋白，並進一步以雙螢光分子雜交技術（BiFC）來確認這些蛋白與 HDA15 的交互作用。其中，我們發現 HDA15 與會參與植物抗病反應的 MOS4 Associated Complex 有交互作用。HDA15 突變株接種 *Pseudomonas syringae* pv. tomato DC3000 3 天後表現出對病原菌敏感，而此一病徵與 *mos4-1* 的表型相似，說明 HDA15 可能參與在植物抗病反應中調控植物的免疫反應。

BIM1，BIM2 和 BIM3 為 bHLH 的成員，會與 BES1 共同作用在 E-box 的啟動子區域上去調控 Brassinosteroid 反應基因。依據先前文獻，*bim1/bim2/bim3* 三重突變會造成 BR 調控基因的反應下降。在本研究中，我們發現 BIM2 會與 HDA15 以及 HDA6 有交互作用。此外，HDA6 與突變株 *bim1/bim2/bim3* 三重突變株在高鹽逆境下會出現花青素累積量下降，以及在種子萌發時期對高鹽逆境敏感的現象。

關鍵字:阿拉伯芥、組蛋白去乙醯酶 HDA15、MOS4 複合體，抗病反應

Abstract

Histone deacetylases (HDACs or HDAs) are responsible for the deacetylation of lysine residues on the N-terminal tail of core histones and play an important role in transcriptional regulation, cell cycle progression and developmental events. HISTONE DEACETYLASES 15 (HDA15), one of the RPD3/HDA1 superfamily members, is known to regulate chlorophyll biosynthesis and photosynthesis by interacting with PHYTOCHROME INTERACTING FACTOR3 (PIF3). We found that many proteins can interact with HDA15 by LC-MS/MS analysis. The interaction of HDA15 with these identified proteins was further confirmed by bimolecular fluorescence complementation assays. In particular, we found that HDA15 can interact with the MOS4 associated complex involved in plant immune responses. Similar to *mos4-1*, *hda15* mutants were hypersensitive to *Pseudomonas syringae* pv. tomato DC3000 after three days inoculation, supporting that HDA15 may interact with the MOS4 associated complex to regulate plant immunity.

BES1-INTERACTING MYC-LIKE PROTEINS 1 (BIM1), BIM2 and BIM3 belong to the bHLH protein family. BIMs interact with BR-INSENSITIVE-EMS-SUPPRESSOR1 (BES1) to synergistically bind to the E-boxes that are present in the promoter regions of a multitude of genes such as Brassinosteroid (BR) responding genes. It was reported that the simultaneous elimination of all three BIM proteins results

in reduced BR-mediated responses. In this study, we found that BIM2 can interact with HDA15 and HDA6, and *bim1/bim2/bim3* and *axe1-5* accumulate less anthocyanin under high salt conditions and are hypersensitive to salt stress in the seed germination stage.

Key words: Arabidopsis, histone deacetylases 15, MOS4 associated complex, plant immunity

Index

Introduction

Histone deacetylases

Histone acetylation/deacetylation mediated by histone acetyltransferases (HATs) and histone deacetylases (HDACs or HDAs) is a reversible process that plays an important role in epigenetic regulation (Fuchs et al., 2006). Histone acetylation occurs at the amino groups of lysine residues within the histone N-terminal tails that protrude out of nucleosomes (Shahbazian and Grunstein, 2007). In plants, the lysine residues 9, 14, 18 and 23 of histonee H3 and the lysine residues 5, 8, 12, 16 and 20 of histone H4 can be acetylated and deacetylated (Fuchs et al., 2006). HATs attach acetyl moiety of acetyl-CoA to the ε-amino group of specific lysine residues on histones and neutralizes the positive charge on the lysine residues. Reduced electrostatic interactions between acetylated histones and phosphate groups of DNA make the DNA more accessible for transcription factor complexes. HDACs remove acetyl group from histones and make opposite effects (Henikoff, 2005; Shahbazian and Grunstein, 2007)

The global protein interaction network for all 11 human HDACs in T cells was reported recently (Joshi et al., 2013). 29 previously unreported putative HDAC1 interactions were identified, 11 of which are implicated in chromatin remodeling and gene expression and 10 of these interactions are zinc finger domain-containing proteins. Zinc finger proteins are known components of chromatin remodeling complexes,

including CoREST (e.g., ZMYM2 and 3) and NuRD (e.g., IKZF1). HDAC1 also co-isolated with WDR5, ARID5B, and PWWP2A, which have been shown either to directly regulate histone methylation or recruit demethylase complexes to histone-bound DNA (Han et al., 2006; Vermeulen et al., 2010; Baba et al., 2011). Among the less well-characterized HDACs, most interactions were found to be unique to distinct HDACs. For example, HDAC8 interacts with components of the cohesin complex, SMC1A, SMC3, and STAG2, involved in sister chromatid segregation during mitosis (Barbero, 2009). Another noteworthy HDAC9 interaction was KIAA1967, known as deleted in breast cancer 1 (DBC1), which was implicated in inhibition of HDAC3 (Chini et al., 2010) and SIRT1, a nicotinamide adenine dinucleotide (NAD+)-dependent deacetylase (Kim et al., 2008; Zhao et al., 2008).

HDAs in plant can be classified into three families, including the RPD3/HDA1-like family, SIR2-like family and HD2 family (Pandey et al., 2002). HDA15 has a RanBP2- type zinc finger (Pandey et al., 2002) and its localization is affected by environment changes. HDA15 is imported into the nucleus in the presence of light, but exported out of the nucleus in the absence of light (Alinsug et al., 2012). Previous studies indicate that PIF3 associates with HDA15 to repress chlorophyll biosynthetic and photosynthetic genes in etiolated seedlings in dark condition (Liu et al., 2013). PIF3 recruits HDA15 to the G-box elements of light-responsive genes to repress their

expression in the dark. On light exposure, the active forms of phytochromes translocated into the nucleus induces rapid phosphorylation and degradation of PIF3, resulting in the dissociation of HDA15 from the targets and activation of the light-responsive genes.

Salt stress response in plants

Salinity is a major environmental stress in plant agriculture worldwide that adversely affects plant growth and metabolism. About 20% of the world's cultivated land and nearly half of all irrigated lands are affected by salinity (Zhu, 2001). At least six signal transduction pathways exist in plants for responding to high salinity, three are ABA dependent and three are ABA independent (Shinozaki and Yamaguchi-Shinozaki, 2007). In the ABA-dependent pathways, AREB/ABFs are bZIP transcription factors involved in this process and trigger *RD29B* and *RD20A* gene expression. MYB2 and MYC2 function in the regulation of ABA-inducible genes such as *RD22*. The NAC transcription factor RD26 is involved in ABA-responsive gene expression in stress responses which trigger *Gly* gene expression. *RD22*, *Gly*, *RD29B* and *RD20A* gene products further regulate salt stress response and tolerance (Shinozaki and Yamaguchi-Shinozaki, 2007).

In ABA-independent pathways, DREB1/CBFs and DREB2 belonging to the

ERF/AP2 family bind to the conserved DNA-binding motif of A/GCCGAC and trigger *RD29A* gene expression. The NAC and HD-ZIP transcription factors are involved in the regulation *ERD1* gene expression (Shinozaki and Yamaguchi-Shinozaki, 2007).

The involvement of HDACs in stress response has been reported. HDA6 and HDA19 can interact with a co-repressor AtSin3 (Chen et al., 2010). AtERF4 and AtERF7 bind to the promoters of the target genes, recruit AtSin3, HDA6 and HDA19 to form a transcription complex and repress gene expression by histone deacetylation (Chen et al., 2010). In the *HDA6* mutant, *axe1-5*, the expression of salt responsive genes, *DREB2A, RD29A,* and *RD29B,* was induced compared with wild type after treatment with 250 mM NaCl (Chen et al., 2010). In addition, the expression of four *HD2* genes, *HD2A, HD2B, HD2C* and HD2D, was reduced after salt treatment (Luo et al., 2012). In addition, *hd2c*mutants showed lower seed germination rates and survival rates under salt stress compared with wild type (Luo et al., 2012). Furthermore, HD2C interacts with HDA6 to modulate salt stress response (Luo et al., 2012).

BES1-INTERACTING MYC-LIKE (BIMs) proteins

Brassinosteroids (BRs) were initially found in the organic solvent extract of pollen from *Brassica napus* and were named brassins. Based on their ability to cause marked changes in growth and differentiation at low concentrations, brassins were classified

into a new family of plant hormones known as brassinosteroids (Mitchell et al., 1970). Brassinosteroids are a group of steroidal hormones that play important roles in plant developmental processes including cell division and cell elongation in stems and roots, photo-morphogenesis, reproductive development, leaf senescence, and response to biotic and abiotic stresses (Choudhary et al., 2012).

BES1-INTERACTING MYC-LIKE proteins (BIMs) belong to the bHLH protein family. BIMs can interact with BR-INSENSITIVE-EMS-SUPPRESSOR1 (BES1) to synergistically bind to the E-boxes that are present in the promoter regions of a multitude of genes (Yin et al., 2005; Guo et al., 2013). BES1 binds the E-box motif through interacting with three BIM transcriptional factors to activate gene expression (Li and Jin, 2007). Recently, it was reported that BR repression of gene expression requires HDA activity (Oh et al., 2014). BR regulates plant development by activating the transcription factor BRASSINAZOLE RESISTANT1 (BZR1) and BZR1 repression of gene expression requires both TOPLESS (TPL) and also activity of HDA that is known to interact with TPL (Oh et al., 2014).

Plant Immunity

Because of plants' sessile lifestyle and lack of mobile cells, they have evolved complex pathogen defense to protect themselves from pathogen attack. When pathogens invade plants, they will release some molecules or structural features such

as pathogen-associated or microbe-associated molecular patterns (PAMPs or MAMPs), that can be recognized by pattern recognition receptors (PRRs) belonging to the receptor-like kinase (RLK) type (Jones and Dangl, 2006). After PRRs recognizing PAMPs, defense genes are induced and PAMP-triggered immunity (PTI) is initiated. However, some bacterial, oomycete or fungal pathogens release effector molecules to inhibit PTI and cause effector-triggered susceptibility (ETS). Subsequently, plants have evolved resistance (R) proteins that can recognize specific effectors and cause effector-triggered immunity (ETI).

Both PTI and ETI can trigger downstream defense gene activation followed by RNA processing steps including 3' polyadenylation, splicing, 5' capping and mRNA export. MAC5A/B associate with the MOS4-associated Complex (MAC, which include MOS4, AtCDC5, MAC 3B and PRL1), and may contribute to mRNA splicing during pathogen defense. When MAC5A/B is associated with MAC complex, MOS11 interacts with mature RNA and export RNA out of the nucleus by the nuclear pore. Once RNA is exported, it would trigger dicer proteins and argonaute (AGO) proteins to do further modification. Dicer-like 2 (DCL2) and Dicer-like 4 (DCL4) are both required in the formation of siRNAs in RNAi. DCL2 is required for siRNA formation for viral RNA silencing, and DCL4 is required for sense transgene-induced RNA-silencing and production of siRNAs for endogenous gene regulation (Xie et al., 2005).

Similarly, argonaute (AGO) proteins (AGO1, AGO2, and AGO7) are also involved in RNAi, they are RNA-binding components of the RNA-induced silencing complex (RISC). AGO proteins directly bind RNA, which allows RISC to either cleave the target RNA to be silenced or prevents translation (Meister, and Tuschi. 2004). Therefore, once recognition occurs, a signaling cascade begins, leading to the activation of downstream genes to mount a robust and quick defense response to prevent pathogens attack plants (Jones and Dangl, 2006).

Based on our liquid chromatography coupled with tandem mass spectrometry (LC-MS/MS) analysis results, our lab found that many proteins can interact with HDA15. The interaction of HDA15 with some of these identified proteins was further confirmed by bimolecular fluorescence complementation assays. In particular, we found that HDA15 can interact with the MOS4 associated complex involved in plant immune responses. Similar to *mos4-1*, *hda15* mutants were hypersensitive to *Pseudomonas syringae* pv. tomato DC3000, supporting that HDA15 may interact with the MOS4 associated complex to regulate plant immunity.

Materials and Methods

Plant Materials

Arabidopsis thaliana ecotype Columbia seeds were germinated and grown at 23 ℃ under long day conditions (16 h light/8 h dark cycle) or short day conditions (8 h light/16 h dark cycle). The loss-of-function mutant, *bim1/bim2/bim3,* is the T-DNA insertion mutant obtaining from Dr. Chory.

Quick DNA extraction

1. Cut one rosette leaf from *Arabidopsis* plants and put into a 1.5 ml tube, and then add 400 µl DNA extraction buffer.
2. Use micropestle to grind the leaf gently, and then incubate in room temperature for 3 minutes.
3. Centrifuge at 12000 rpm for 5 minutes. Then, transfer 300 µl supernatant into a new tube.
4. Add the equal volume of isopropanol and mixed it well.
5. Centrifuge at 12000 rpm for 5 minutes.
6. Remove the supernatant and add 200 µl of 75% ethanol to wash the DNA pellet.
7. Centrifuge at 12000 rpm for 5 minutes again.
8. Discard the 75% ethanol and air dry the DNA pellet. Dissolve the pellet in 50 µl

sterile distilled water.

RNA isolation

1. 0.1~0.2 g of *Arabidopsis thaliana* leaves were ground into fine powder with liquid nitrogen, and then mixed with 1 ml of TROZOL Reagent (Invitrogen; catalogue no. 15596-018).
2. The resulting solution was transferred to 1.5 ml tube and further incubated for 5 minutes at room temperature to permit complete dissociation of nucleoprotein complexes.
3. 200 μl of chloroform per 1 ml of TROZOL Reagent was added into the extraction mixture. Shake the tubes vigorously by hand for 15 seconds and incubated for 3 minutes at room temperature.
4. The sample was centrifuged at 12000 g at 4℃ for 15 minutes.
5. Following centrifugation, the mixture was separated into a lower red phenol-chloroform phase, an interphase, and a colorless upper aqueous phase. RNA remained exclusively in the aqueous phase, and the volume of the aqueous phase was about 70% of the volume of TROZOL Reagent used for homogenization.
6. The aqueous phase was transferred to a new tube, and RNA was then precipitated form the aqueous phase by mixing with equal volume of isopropyl alcohol.
7. The samples were further incubated at the room temperature for 10 minutes and

centrifuged at 12000 g at 4℃ for 10 minutes.

8. Following centrifugation, the supernatants were removed and the RNA pellets were washed once with 1 ml of 70% ethanol (DEPC-treated water prepared).
9. The sample were mixed and then centrifuged at 7500 g at 4℃ for 5 minutes.
10. Following centrifugation, the supernatant was removed and the remaining pellets were air-dried briefly for 5 to 10 minutes.
11. RNA was dissolved with 35 μl DEPC-treated water and incubated at 65℃ for 5 minutes.
12. 8 μl RNA sample was added 1 μl of 10X DNase buffer and 1 μl of DNase (Promagal Catalogue no. M6101) and then incubated at 37℃ for 30 minutes to remove residual DNA.
13. 1 μl of stop solution was added into RNA sample to stop the reaction of DNase treatment, and incubated at 65℃ for 10 minutes.
14. Finally, the RNA sample was stored in a -20℃ freezer.

RT-PCR analysis

1. 3 μg of RNA in a sterile RNase-free 1.5 ml tube was heated to 65℃ for 5 minutes to melt secondary structure and the tube was cooled down immediately on ice to prevent secondary structure form reforming.

2. The tube was spun briefly to collect the solution at the bottom of the tube.
3. The following components were added to the tube: 4 μl of M-MLV (Moloney Murine Leukemia Virus) 5X RT buffer (Promega; Catalogue no. M531A), 4 μl of 2.5 mM dNTP (dATP, dCDP, dGDP, dTTP), 3 μl of 5 mM oligo (dT), 1 μl of M-MLV reverse transcriptase (Promega; Catalogue no. M170B), 1 μl of recombinant RNasin ribonuclease inhibitor (Promega; Catalogue no. N251B), and added DEPC-treated water to total volume 20 μl.
4. The solution was mixed gently by flicking the tube and incubated for 60 minutes at 37℃, and then diluted the cDNA solution with 20 μl of sterile distilled water.

Quantitative real-time PCR (qPCR)

100X diluted cDNA obtained from RT-PCR were used as a template to run real-time PCR. The following components were added to a reaction tube: 9 μl of iQ™ SYBR Green Supermix solution (Bio-Rad; Catalogue no. 170-8882), 1 μl of 5 μM specific primers and 8 μl of the diluted template. *Ubiquitin* was used as an internal control in real-time quantitative RT-PCR. Real-time PCR experiments were performed in triplicate. Thermocycling conditions were 95℃ for 3 minutes followed by 40-50 cycles of 95℃ for 30 seconds, 60℃ for 30 seconds, and 72℃ for 20 seconds, with a melting curve detected at 95℃ for 1 minute, 55℃ for 1 minute and detected the

denature time from 55℃ to 95℃. The gene-specific primer pairs are listed in Table 4.

Seed germination in Petri dishes

Before germination in Petri dishes, all seeds were treated with 50% bleach solution and 0.02% Triton-X-100 for 10 minutes to sterilize and washed with distilled water three times to remove the bleach. The sterilized seeds were incubated at 4℃ for three days to promote germination, and then plated on Petri dishes containing different growth media. The media contained 1/2MS salt, 1% sucrose, 1% agar and were supplemented with or without NaCl. All plants were transferred to growth chamber and incubated at 23℃ under long day condition (16 h light/8 h dark cycle).

Measurement of germination rates

The sterilized seeds were incubated at 4℃ for 3 days before growing in Petri dishes. For germination rate analysis, seeds were germinated on 1/2MS medium with or without different concentrations of NaCl (125 mM, 150 mM and 175 mM) in growth chambers, and seed germination rates were analyzed after 2 days.

Bimolecular Fluorescence Complementation (BiFC) assay

A. Plasmids construction

To generate the construct for BiFC assay, full length coding sequences of BIM2,

HDA15 related proteins, and HDA15 were PCR amplified. The resulting PCR products were first sub cloned into the pCR8/GW/TOPO vector, and then recombined to the pEarleyGate201-YN and pEarleyGate202-YC vector (Lu et al., 2010). Pfu polymerase (FINNZYMES; Catalogue no.F530S) was used in the PCR reaction to minimize undesired mutations in the sequences, and the resulting constructs were sequenced and confirmed by the Vector NTI Suite program (InforMax Inc., Bethesda, MD, USA).

B. Protoplast isolation

1. 10 ml of the fresh enzyme solution was prepared with heat activation at 55℃ for 10 minutes.
2. After cooling the enzyme solution to room temperature, 100 µl of 1 mM $CaCl_2$ and 100 µl of 10% BSA were added to the enzyme solution.
3. Leaves were cut into small pieces and their lower epidermis were removed, and then soaked in the enzyme solution.
4. The digestion was carried out for 1.5 hours in light with gently shaking at 50 rpm.
5. The solution was transferred into a 5 ml tube and centrifuged at 100 g for 3 minutes.
6. Supernatant was removed, and protoplasts were washed twice by 4 ml of W5 buffer with centrifugation at 100 g for one minute.
7. The protoplasts were dissolved in another 2~5 ml of W5 buffer.
8. The protoplasts were kept on ice for 30 minutes before transfection.

Enzyme solution

Reagent	Amount	Final concentration
Cellulase R10	0.15 g	1%
Macerozyme R10	0.03 g	0.25%
0.8 M Mannitol	5 ml	0.4 M
0.2 M KCl	1 ml	20 mM
0.1 M MES	2 ml	20 mM
Water	To 10 ml	

W5 Buffer

Reagent	Amount	Final concentration
3 M NaCl	10.3 ml	154 mM
1 M $CaCl_2$	25 ml	125 mM
0.2 M KCl	5 ml	5 mM
0.1 M MES	4 ml	2 mM
0.1 M glucose	10 ml	5 mM
Water	To 200 ml	

C. Protoplast Polyethylene glycol (PEG) transfection

1. The W5 buffer was removed by centrifugation at 100 g for one minute, and the protoplasts were resuspended in an equal volume of MMg solution.
2. For 200 µl of protoplasts (~$4*10^5$), 20 µl of plasmid DNA (20-40 µg) was added in a 5 ml tube and mixed well.
3. Added 220 µl of PEG/Ca solution (final PEG concentration = 20%) and mixed well.
4. The tube was incubated at 23℃ for 5 minutes.
5. The protoplast solution was diluted with 2 ml of W5 buffer and centrifuged at 100 g for one minute to remove PEG.

6. The protoplasts were washed twice by 4 ml of W5 buffer with centrifugation at 100 g for one minute.
7. The protoplasts were dissolved in another 100 μl of W5 buffer.
8. The protoplasts were incubated under light. The fluorescent signal could be seen after 16~22 hours.

MMg solution

Reagent	Amount	Final concentration
0.8 M Mannitol	5 ml	0.4 M
1 M $MgCl_2$	0.15 ml	15 mM
0.1 M MES	0.4 ml	4 mM
Water	to 10 ml	

PEG/Ca solution

Reagent	Amount	Final concentration
PEG4000	2 g	40%
0.8 M Mannitol	1.25 ml	0.2 M
1 M $CaCl_2$	0.5 ml	0.1 M
Water	to 5 ml	

Anthocyanin accumulation assays (Bate and Rothstein, 1998)

The sterilized seeds were incubated at 4℃ for 3 days before growing in Petri dishes. For anthocyanin accumulation analysis, seeds were germinated on 1/2 MS media in growth chambers for 4 days, and transferred to 1/2 MS with or without salt (0, 125 mM, 150 mM NaCl) growth for 14 days.

For anthocyanin analysis, frozen plant tissues were ground in 1.5 ml microfuge

tubes with a disposable pestle, and total plant pigments were extracted overnight in 0.3 ml of 1% HCl in methanol. After the addition of 0.2 ml of H2O, chlorophyll was separated from the anthocyanin by extraction with an equal volume of chloroform. The quantity of anthocyanin was determined by spectrophotometric measurements by taking readings at the wavelengths of 530 nm and 657 nm. The total Anthocyanin content was calculated with using the formula: (A530-0.33A657)/g of fresh weight.

Pathogen inoculation (Zimmerli et al., 2001)

For the bacterial pathogen *Pseudomonas syringae* pv. tomato DC3000, five-week-old Arabidopsis plants were dipped in a bacterial suspension of 10^6 colony-forming units (CFU)/mL *Pst* DC3000 in 10 mM $MgSO_4$ containing 0.01% Silwet L-77 (Lehle Seeds) for 15 min. After dipping, plants were kept at 100% relative humidity overnight. Disease symptoms were evaluated at 3 days post inoculation (dpi).

For bacterial titers, leaf discs collected at 2 dpi were washed twice with sterile water and homogenized in 10 mM MgSO4. Quantification was done by plating appropriate dilutions on LB agar containing rifampicin (50mg/liter) as previously described (Zimmerli et al., 2001). Each biological repeat represents nine leaf discs (0.6 cm diameter) from three different plants.

Results

Identification of HDA15 interaction proteins

LC/MS-MS analysis was performed to identify HDA15 interaction proteins. We generated HDA15 antibody-resin to immunoprecipitate endogenous HDA15 protein complexes in Col plants and used GFP-Trap magnetic beads to immunoprecipitate

HDA15-GFP in *hda15-1* mutant transgenic plants expressing *35S:HDA15-GFP* in etiolated seedlings. HDA15 may interact with chromatin-related proteins, transcription factors and proteins involved in various developmental pathways (Table1).

LC/MS-MS analysis revealed that HDA15 may interact with histone acetyltransferase, histone methyltransferase, DNA methyltransfrases, AGO proteins and chromatin remodeling proteins (Table 1). In particular, we found that HDA15 can interact with two histone demethylases, LDL1 and FLD. The interaction of HDA15 and LDL2 was further confirmed by BiFC assays in tobacco leaves (Figure 1).

LC/MS-MS analysis indicated that HDA15 can interact with various transcription factors including MADS-box proteins, WRKY proteins, Basic Helix-Loop-Helix Dimerrisation Region (bHLH) proteins, MYB DNA binding proteins, ARF family proteins and NAC family proteins (Table 2). By using BiFC assays, we further confirmed that HDA15 can interact with AGL72, AGL79, bHLH99, ICE1 and CDC5 in tobacco leaves (Figure 2).

Other HDA15 interacting proteins identified by LC/MS-MS analysis are involved in response to hormone, abiotic stress and light stimulus (Supplementary Table 1). In addition, HDA15 also interacted with ubiquitin ligases, kinases, zinc finger proteins, WD40/YVTN repeat-like proteins, DNA/RNA-binding proteins, peroxidases ribosome related proteins, and iron binding proteins. The interaction of HDA15 with TIFY8 and

MAC3B was confirmed by BiFC assays (Figure 3).

The HDA15 interacting proteins were classified into several groups according to their functional categories (Figure 4). These proteins are involved in abiotic stress responses, flowering time control, circadian rhythm regulate, and light response. The MAC (MOS4-Associated Complex) complex is involved in plant defense. We found that HDA15 can interact with MAC complex members, CDC5, MAC3B and SE in BiFC assays. MOS4 is the core protein in MAC complex (Monaghan et al., 2009). By using BiFC assays, we found that MOS4 can also interact with HDA15 in Arabidopsis protoplasts (Figure5).

We found that BIM2 and ALC can interact with HDA15 (Figure 6 A and 6B). In addition, the subcellular localization of BIM2 and ALC is in the nucleus (Figure 7). Take these BiFC assays result together, HDA15 may interact with many proteins to co-regulate plant development and phenomena.

The *hda15* mutant is hyposensitive to salt stress in seed germination

LC-MS/MS analysis revealed that HDA15 interacts with proteins involved in abiotic stress, suggesting that HDA15 may play a role in stress response. Therefore, we tested to evaluate if *hda15-1* has any phenotype under salt stress during seed germination. At 150 mM NaCl, the seed germination rate of *hda15-1* was higher compared to Col-0 (Figure 8). In contrast, the seed germination rate of the *had6* mutant,

axe1-5 was reported to hypersensitive to salt stress is used for negative control , is lower compared to Col-0 indicate that HDA15 and HDA6 may involve in plant stress response in seed germination stage, but they may involve in different salt stress regulation pathway.

The *hda15* mutant is hypersensitive to *Pst* DC3000

To evaluate whether HDA15 is involved in pathogen response, the response of the *hda15* mutant to hemi-biotrophic bacterium *Pseudomonas syringae* pv. tomato DC3000 (*Pst* DC3000) was analyzed. *hda15-1* and *hda15-2* contained a higher titer of bacteria at 2 dpi compared to Col-0 (Figure 9B), indicating that *hda15* mutants are hypersensitive to Pst DC3000. On the fourth day after inoculating with *Pst* DC3000, *hda15-1* and *hda15-2* developed more necrosis and bacteria-mediated leaf yellowing compared with Col-0 (Figure 9A). Similarly, *mos4* mutants are also hypersensitive to pathogens (Monaghan et al., 2009). Therefore, HDA15 may interact with the MAC complex to co-regulate the plant immunity. It remains to be determined whether HDA15 act with the MAC complex to regulate plant pathogen defense.

***bim1/bim2/bim3* triple mutant is hypersensitive to salt stress during seed germination**

Previous studies indicated that BIMs are positive regulators in BR signaling

(Belkhadir and Jaillais 2014). It was reported that BIM1, BIM2 and BIM3 are functionally redundant (Yin et al., 2005). The phenotype of *hda15-1* and *bim1/bim2/bim3* triple mutants under salt stress was analyzed. When seeds were grown at media with 125 mM and 150mM NaCl, the seed germination rate of *hda15-1* was higher than Col-0. In contrast, the seed germination rate of the *bim1/bim2/bim3* triple mutant was lower compared to Col-0 (Figure 10).

bim1/bim2/bim3 triple mutant accumulates less anthocyanin

Previous studies indicated that BIMs (BIM1, BIM2 and BIM3) play a positive role in BR signaling and BR is involved in anthocyanin synthesis (Belkhadir and Jaillais, 2015). When treated with different salt concentrations, the *bim1/bim2/bim3* triple mutant not only showed a hypersensitive phenotype during the seed germination stage but also accumulated less anthocyanin (Figure 11 A).

The anthocyanin accumulation in the *bim1/bim2/bim3* triple mutant under salt stress was analyzed. After treating with 150 mM NaCl for two weeks, Col-0 and *hda15-1* accumulated more anthocyanin compared to *bim1/bim2/bim3* and *axe1-5* suggest that BIMs and HDA6 may regulate anthocyanin accumulation in salt stress (Figure 11 B). It remains to be determined whether BIMs interacts with HDA6 to regulate anthocyanin accumulation under salt stress.

To further evaluate the interaction of BIMs and HDA6, the quadruple mutant *axe1-5/bim1/bim2/bim3* (hereafter referred to as *axe1-5/bim123*) was generated by crossing *bim1/bim2/bim3* and *axe1-5*. After treating with 150 mM NaCl for two weeks, Col-0 and *hda15-1* accumulated more anthocyanins compared to *bim1/bim2/bim3, axe1-5,* and *axe1-5/bim123* (Figure 11 C), suggesting that BIMs and HDA6 may involve in the same pathway regulating anthocyanin biosynthesis.

Discussion

Previously, it was reported that HDA15 can interact with PIF3 and co-regulate gene expression in chlorophyll biosynthesis and photosynthesis (Liu et al., 2013). By using LC-MS/MS analysis, we found that HDA15 may interact with many proteins involved in different development pathways. These HDA15-interacting proteins were classified into eight functional groups including abiotic stress responses, flowering time control, circadian rhythm regulation, and light response.

We found that HDA15 interacts with ICE1 (INDUCER OF CBF EXPRESSION1) and RCF3 (REGULATOR OF CBF GENE EXPRESSION 3). ICE1 is a transcription factor that binds to the *CBF3* promoter and is required for activation of *CBF3* expression upon cold stress (Chinnusamy et al., 2003). RCF3 was reported to be involved in heat stress regulation (Guan et al., 2013). It negatively regulates the expression of *HSF* (*HEAT STRESS FACTOR*) genes including *HSFA1a, HSFA1b* and *HSFA1d* and positive regulates the expression of *HSFA1e*, *HSFA3*, *HSFA9*, *HSFB3*, and *DREB2C* (Guan et al., 2013). However, the function of HDA15 in plant thermotolerance regulation is still unclear.

In human cells, the SIN3 complex is composed of the histone deacetylases HDAC1 and HDAC2, two histone-binding proteins RbAp46 and RbAp48, SIN3, SAP18 and SAP30 (Ahringer, 2000). In Arabidopsis, it was reported that SAP18 is

involved in salt stress regulation, since its knockout mutant *sap18-1* shows hypersensitive to salt treatment (Song and Galbraith, 2006). SAP18 can interact with HDA19 and ERF3 to form a repression complex (Song and Galbraith, 2006). According to our LC-MS/MS analysis, we found HDA15 may interact with SAP18 and SIN3, suggesting that HDA15 may also form a complex with SAP18 and SIN3 to co-regulate gene expression in plant stress response.

HDA15 interacts with proteins such as SVP, AP1 and AGL28 involved in flowering time regulation. Furthermore, HDA15 also interacts with EPR1, CCR1 and LUX. LUX is one of circadian related proteins involved in evening loop (McClung. 2011). It can not only positive regulates *CCA1* and *LHY* but also represses *PRR9* with ELF3 and ELF4 (McClung. 2011). It was reported that HDA6 can interact with TPL and PRR9 to repress *CCA1* gene expression (Wang et al., 2013). Furthermore, HDA6 can also interact with FLD to regulate flowering (Yu et al., 2011). Further research is required to investigate whether HDA15 can act coordinately with HDA6 to regulate the circadian rhythm and flowering.

The MOS4-associated Complex (MAC) containing MOS4, CDC5, MAC3, MAC5 and PRL1 was reported to be involved in the regulations of pathogen defense in Arabidopsis (Woloshen et al., 2010). Previously, it was shown that SNC1 (SUPPRESSOR OF NPR1-1, CONSTITUTIVE 1) reduces the nuclear R protein pool

and attenuates the activation of downstream defense responses (Li et al., 2001; Zhang et al., 2003). Furthermore, the *snc1* mutation leads to auto-activation of the R protein and enhanced disease resistance (Li et al., 2001; Zhang et al., 2003). *mos4* (*modifier of snc1, 4*) completely abolishes the enhanced resistance to the virulent pathogens in *snc1* (Palma et al., 2007). We tested the pathogen resistance of *hda15* mutants and found that *hda15* has the similar phenotype as the *mos4* mutant in pathogen response (Monaghan et al., 2009). Both *hda15-1* and *hda15-2* are hypersensitive to *Pst* DC3000. Taken together, these results indicate that HDA15 may interact with the MAC complex involved in plant pathogen immunity.

Brassinosteroids play important roles in plant developmental processes including cell division and cell elongation in stems and roots, photo-morphogenesis, reproductive development, and leaf senescence as well as biotic and abiotic stress responses (Choudhary et al., 2012). It has been reported that BES1 interacts with BIMs to synergistically bind the E-boxes that are present in the promoter regions of a multitude of genes. BES1-BIM complexes are thought to promote the expression of BR-responsive genes (Yin et al., 2005; Yu et al., 2011; Guo et al., 2013). Furthermore, BIM1, BIM2 and BIM3 are functionally redundant and the simultaneous elimination of all three BIM proteins results in reduced BR-mediated responses (Li, 2005). BR induces the expression of *12-OXO-PHYTODIENOIC ACID REDUCTASE 3* (*OPR3*)

under a variety of stimuli such as UV light, touch, wind or wounding. OPR3 is a key enzyme involve in JA biosynthesis. BR may influence the stress response of plants through stimulation of JA biosynthesis (Müssig et al., 2000; Schaller et al., 2000). BR may regulate the JA-induced anthocyanin accumulation through BR signaling, since JA-induced anthocyanin accumulation is reduced in BR mutants or in wild type treated with brassinazole, an inhibitor of BR biosynthesis (Peng et al., 2011).

In this study, we found that the *bim1/bim2/bim3* triple mutant accumulated less anthocyanin in high saline conditions. This may be caused by reducing BR-mediated responses of *bim1/bim2/bim3,* which further represses the JA-induced anthocyanin accumulation. In seed germination assays, *bim1/bim2/bim3* showed hypersensitive to NaCl treatment and accumulated less anthocyanins compared to wild type. On the other hand, *axe1-5* also accumulated less anthocyanin accumulation and was hypersensitive to salt in seed germination assays. Further research is required to investigate the molecular mechanisms of the interaction of HDA6 and BIMs and their involvement in abiotic stress response.

Figures

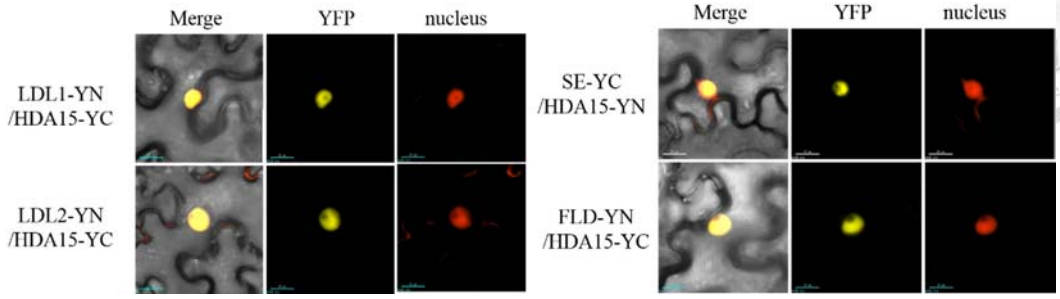

Figure 1. HDA15 interacts with chromatin-related proteins.

BiFC assays were carried out in tobacco leaves to detect the interaction of HDA15 with LDL1, LDL2, SE and FLD. HDA15 and other proteins were fused with N-terminal (YN) and C-terminal (YC) of YFP, and were co-transfected into tobacco leave, and visualized using confocal microscope.

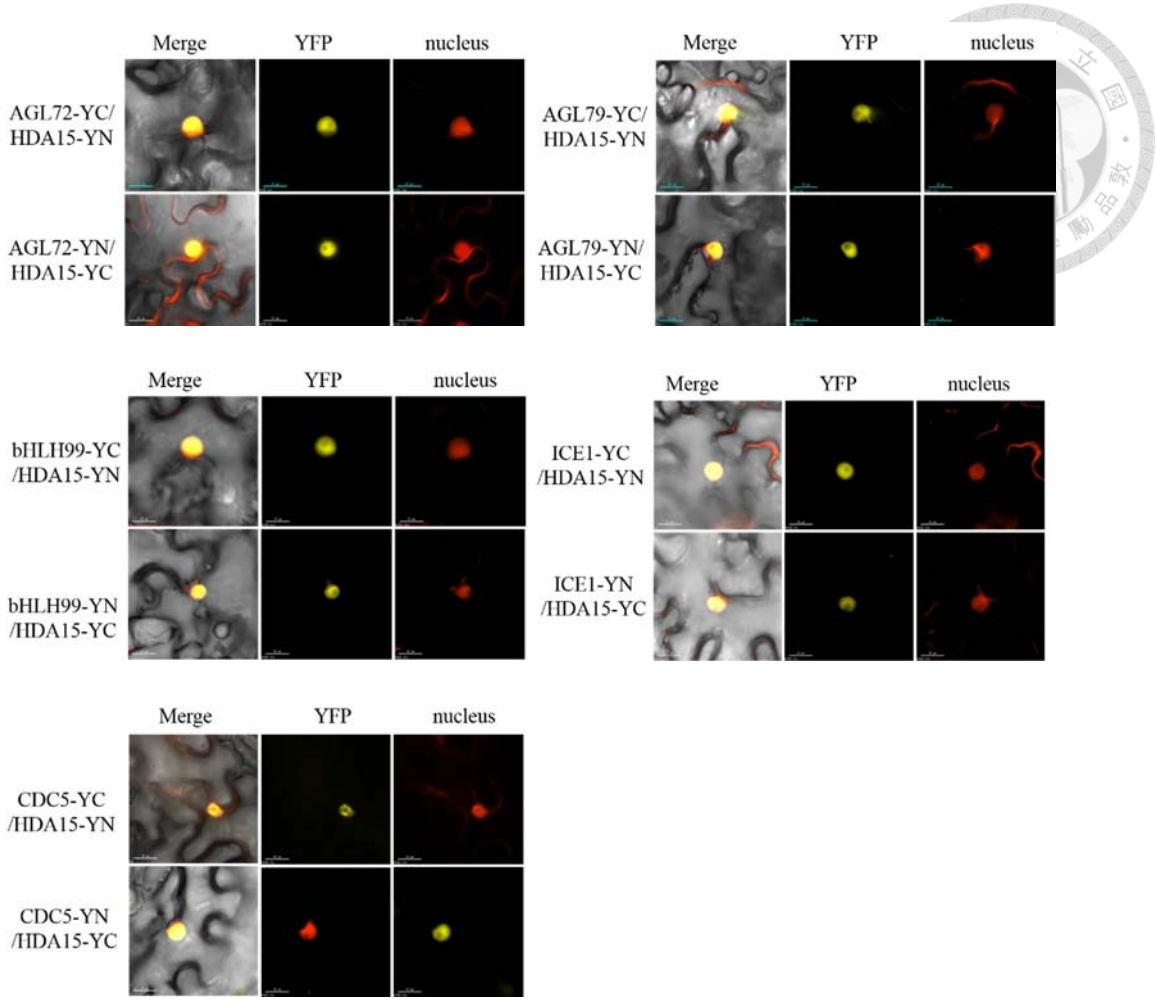

Figure 2. HDA15 interacts with several transcripton factors.

BiFC assays were carried out in tobacco leaves to detect the interaction of HDA15 with AGL72, AGL79, bHLH99, ICE1 and CDC5. HDA15 and other proteins were fused with N-terminal (YN) and C-terminal (YC) of YFP, and were co-transfected into tobacco leave, and visualized using confocal microscope.

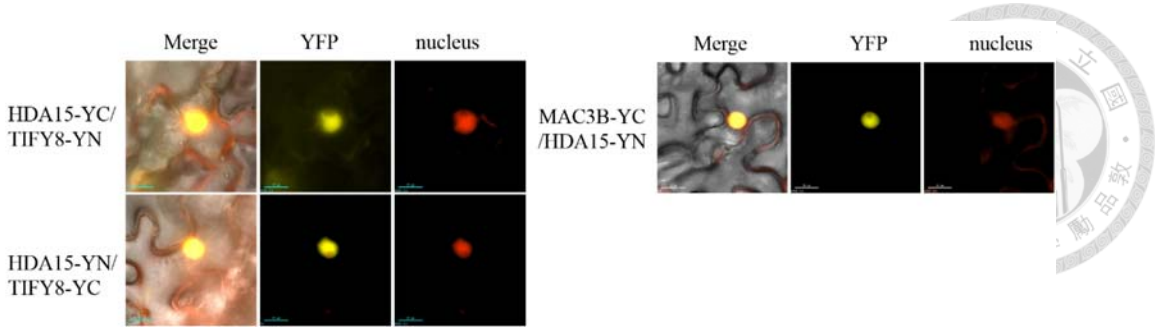

Figure 3. HDA15 interacts with TIFY8 and MAC3B.

BiFC assays were carried out in tobacco leaves to detect the interaction of HDA15 with TIFY8 and MAC3B. HDA15, TIFY8 and MAC3B were fused with N-terminal (YN) and C-terminal (YC) of YFP, and were co-transfected into tobacco leave, and visualized using confocal microscope.

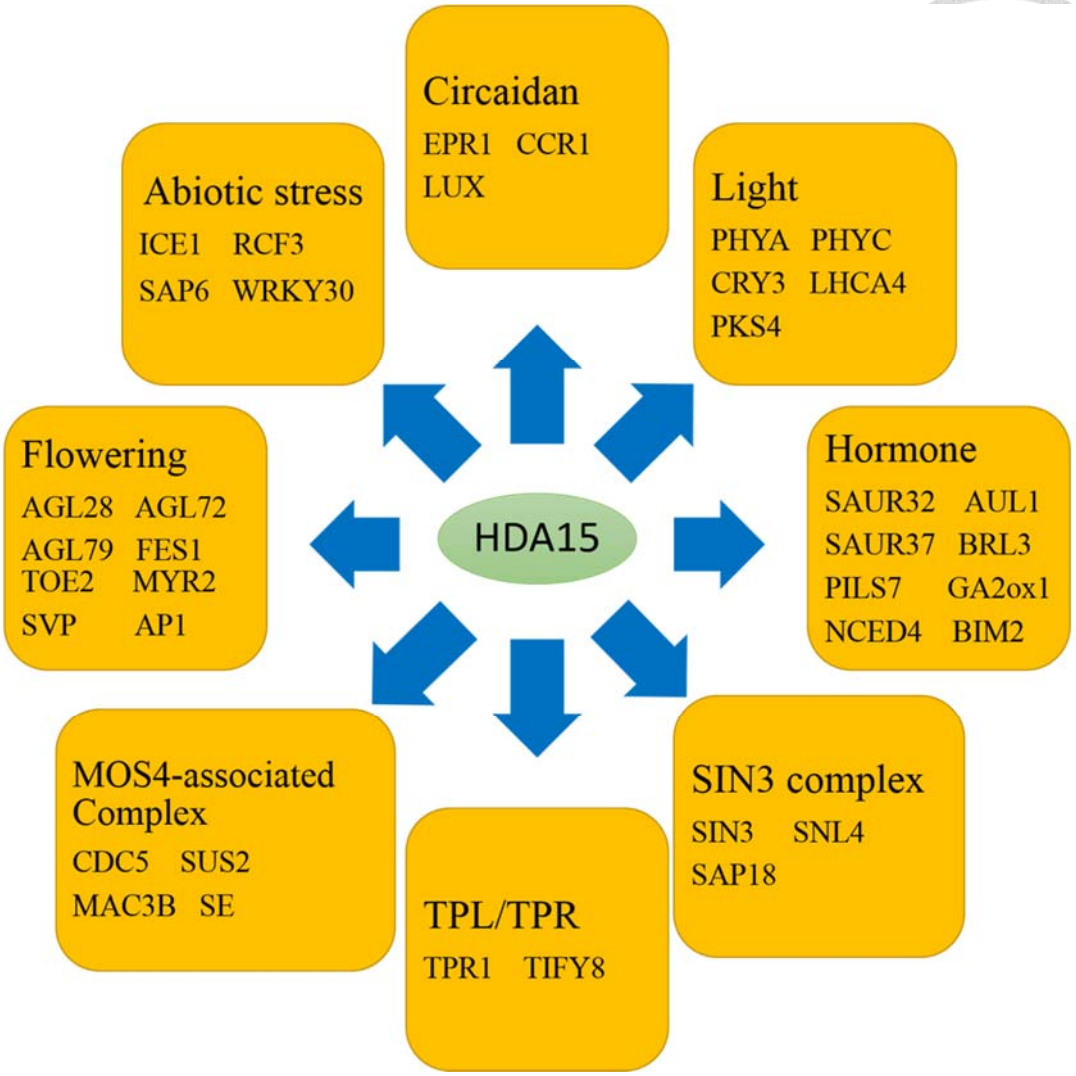

Figure 4. HDA15 interacts with proteins involved in different developmental pathways in Arabidopsis.

HDA15-interacting proteins can be classified into eight categories: abiotic stress related proteins, circadian related proteins, light related proteins, hormone related proteins, SIN3 complex members, TPL/TPR proteins, flowering related proteins, and MOS4-associated complex (MAC) members.

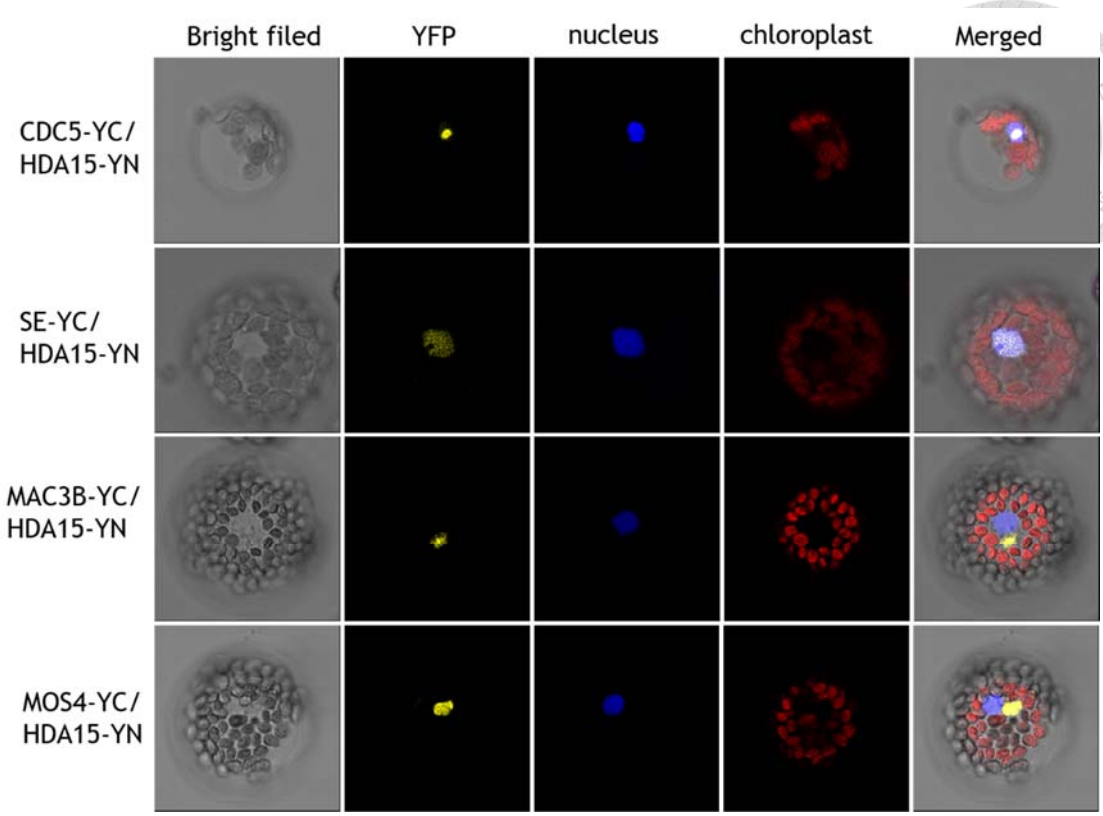

Figure 5. HDA15 interacts with MAC complex members.

BiFC assays were carried out in Arabidopsis protoplasts to detect the interaction of HDA15 with CDC5, SE, MAC3B and MOS4. HDA15 and other proteins were fused with N-terminal (YN) and C-terminal (YC) of YFP, and were co-transfected into tobacco leave, and visualized using confocal microscope.

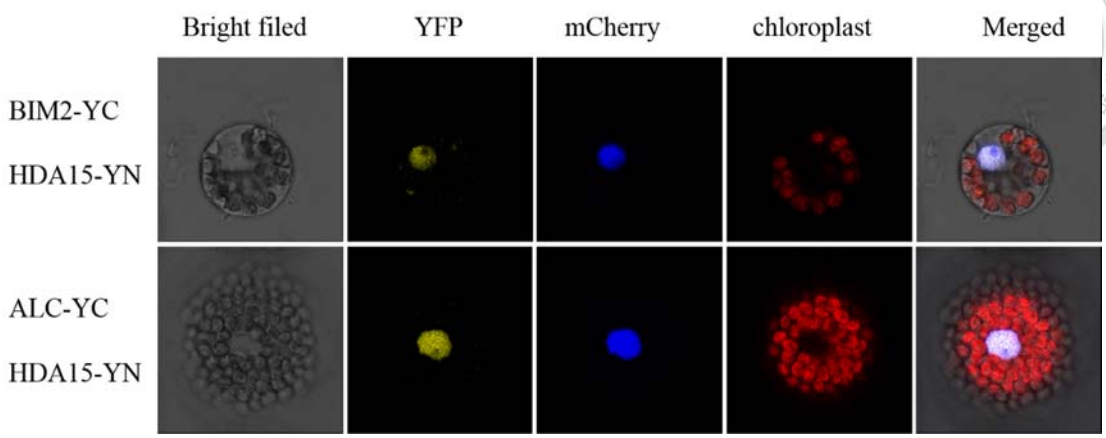

Figure 6. HDA15 interacts with BIM2 and ALC.

BiFC assays were carried out in Arabidopsis protoplasts to detect the interaction of HDA15 with BIM2 and ALC. HDA15, BIM2 and ALC were fused with N-terminal (YN) and C-terminal (YC) of YFP, and were co-transfected into Arabidopsis protoplasts, and visualized using confocal microscope.

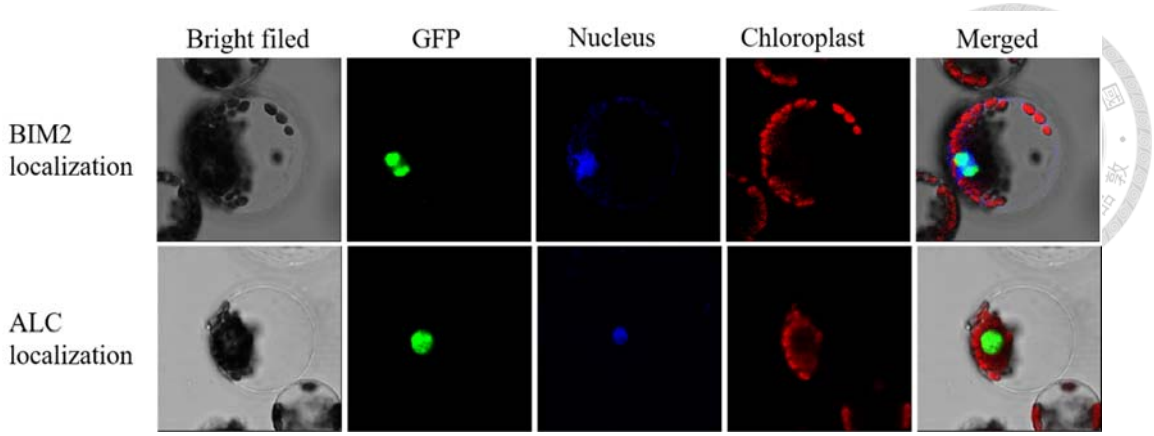

Figure 7. Subcellular localization of BIM and ALC in *Arabidopsis* protoplasts.

BIM2 and ALC fused with GFP were transfected into *Arabidopsis* protoplasts and visualized using confocal microscope.

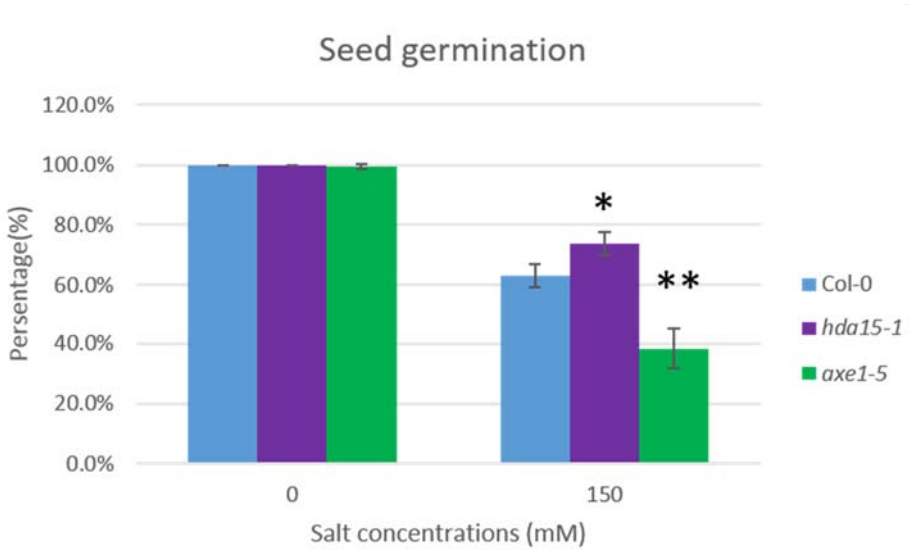

Figure 8. Germination rates of Col-0, *hda15-1,* and *axe1-5* under salt stress.

Seeds were germinated on 1/2 MS media with or without 150 mM NaCl for 3 days. Data are means ± SD of three independent biological replicates ($n \geq 60$). **, $P<0.01$ and *, $P<0.05$, Student's t test.

(a)

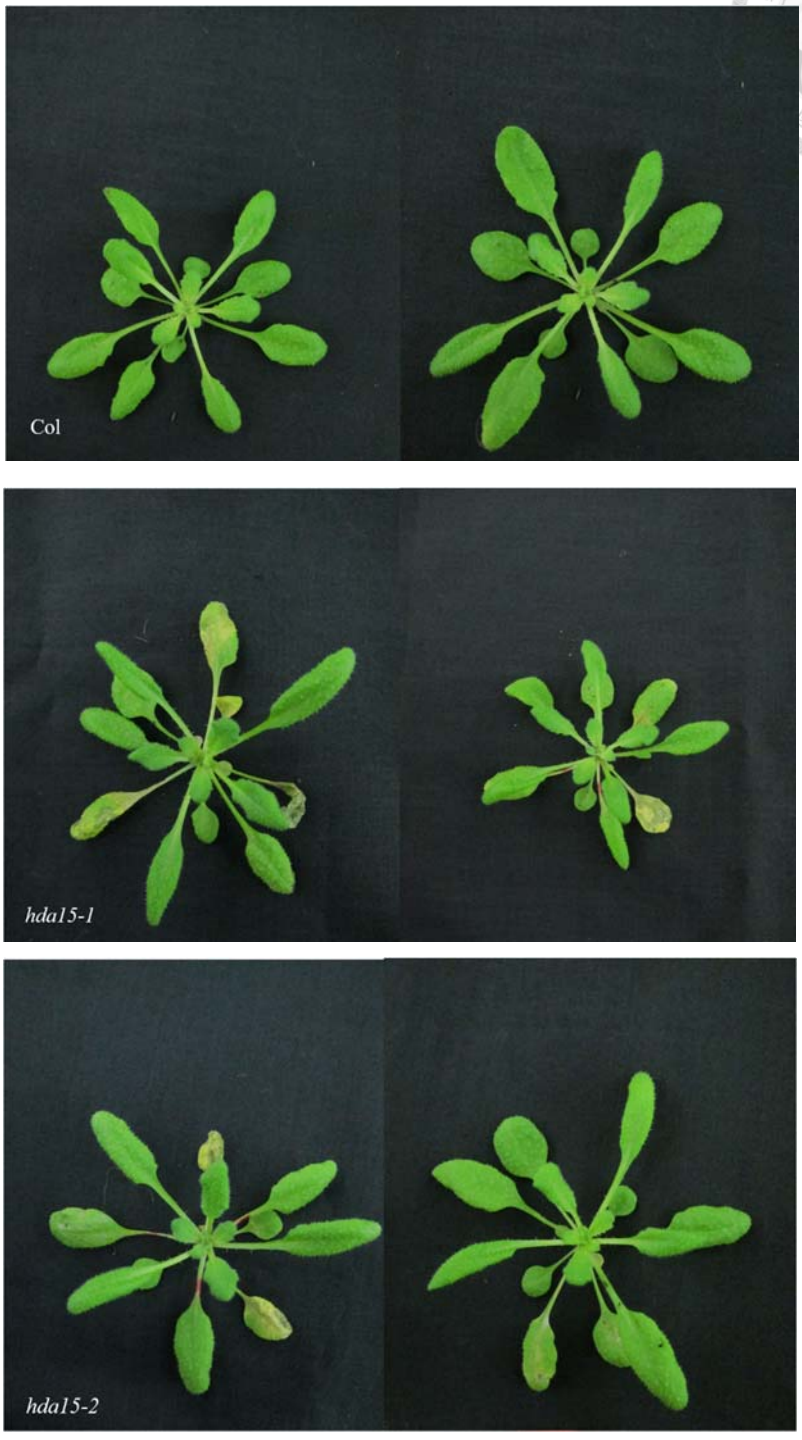

(b)

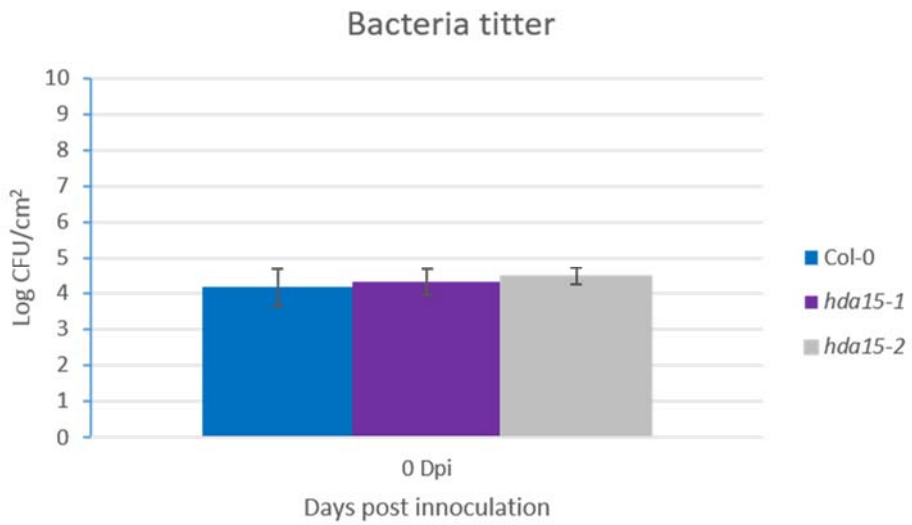

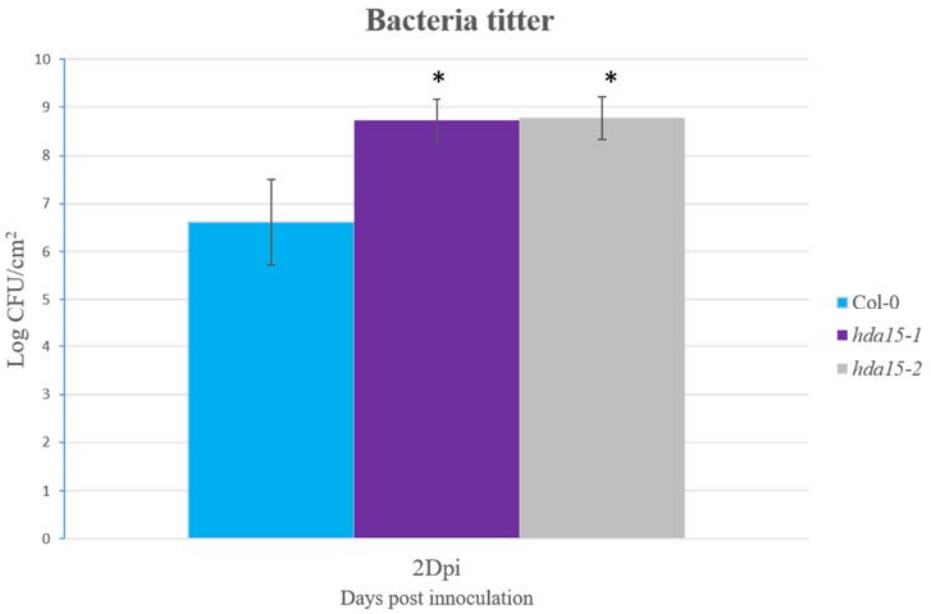

Figure 9. Disease symptom Col-0 and *hda15* mutant lines infected with *Pst* DC3000.

(a) Five-week-old Arabidopsis Col-0 and *hda15* plants were dip-inoculated with 1 × 10^6 cfu/mL *Pst* DC3000. Photos were taken after 4 days. This experiment was repeated at 3 times with similar results. Photos were taken after 3 days

(b) Col-0, *hda15-1* and *hda15-2* were dip-inoculated with 1×10^6 cfu/mL *Pst* DC3000 and bacterial titers were evaluated 0 and2 days later. *, P<0.05, Student's t test.

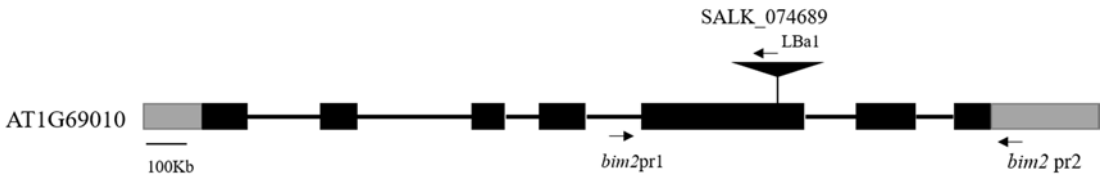

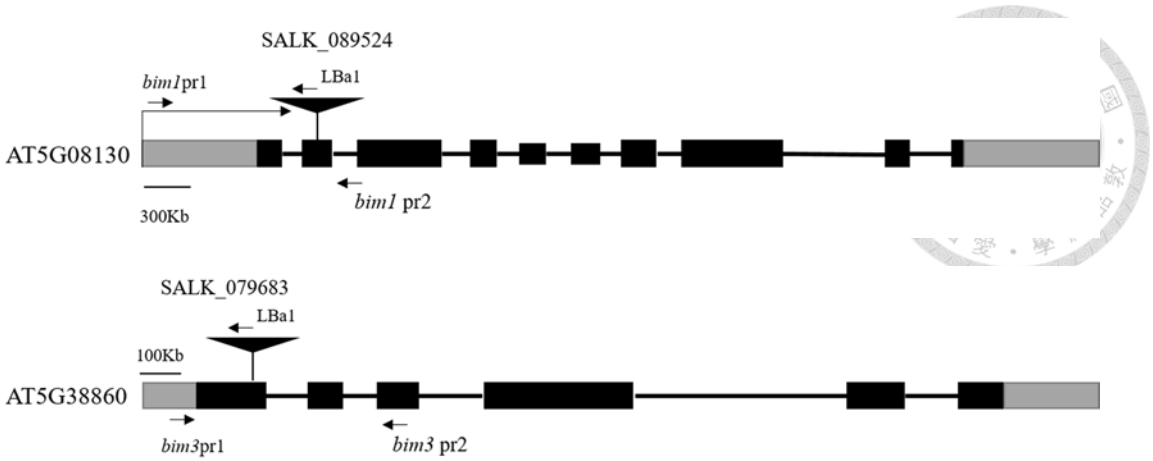

Figure 10. T-DNA insertion sites of *bim1/bim2/bim3* mutants.

Schematic representation of *bim1*, *bim2* and *bim3* alleles. Inverted triangles and arrows indicate T-DNA insertion sites and gene-specific primers, respectively.

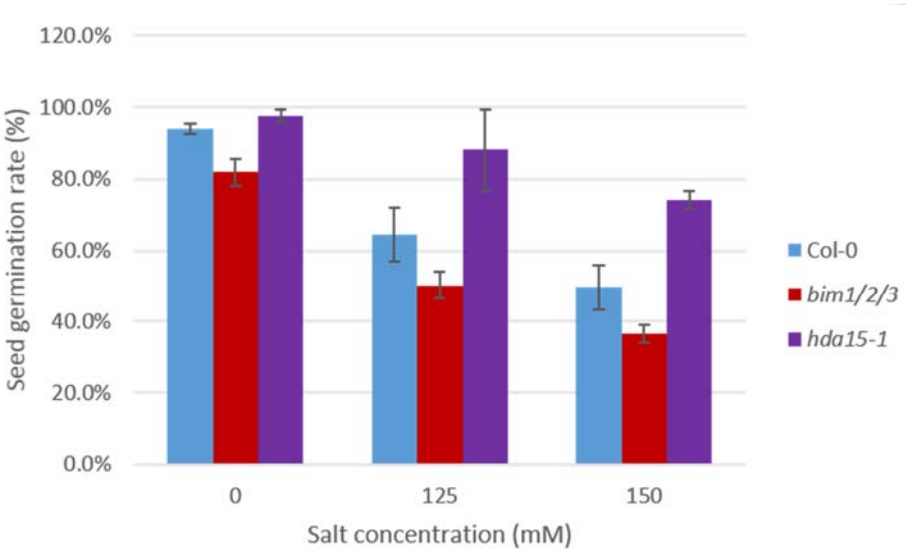

Figure 11. Germination rates of Col-0, *hda15-1,* and *bim1/bim2/bim3* under salt stress.

Seeds were germinated on 1/2 MS media with or without 150 mM NaCl for 3 days.

Data are means ± SD of three independent biological replicates ($n \geq 60$).

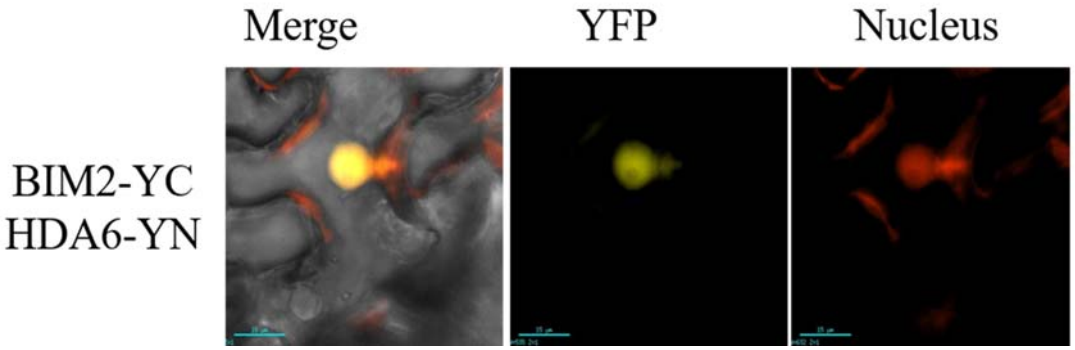

Figure 12. BiFC assays of HDA6 interacting with BIM2 in and tobacco leaves.

Interaction of HDA6 with BIM2. HDA6 and BIM2 fused with N-terminal (YN) and C-terminal (YC) of YFP were co-transfected into tobacco leaves, and visualized using confocal microscope.

(A)

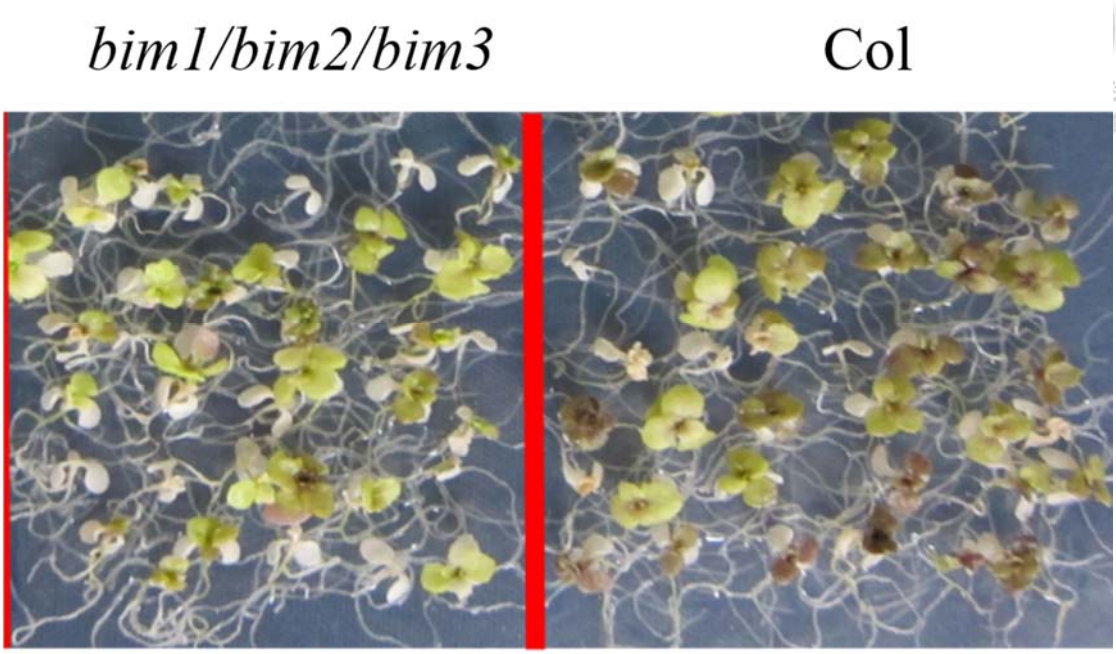
bim1/bim2/bim3
Col

(B)

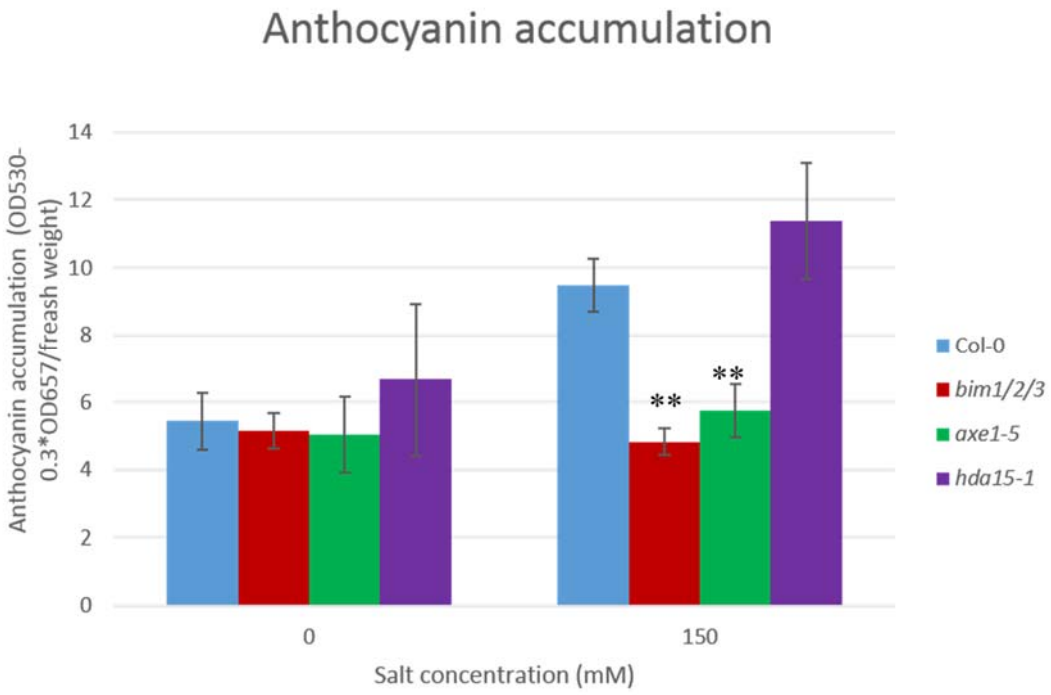
Anthocyanin accumulation
Anthocyanin accumulation (OD530-0.3*OD657/freash weight)
14
12
10
8
6
4
2
0
**
**
0
150
Salt concentration (mM)
Col-0
bim1/2/3
axe1-5
hda15-1

(C)

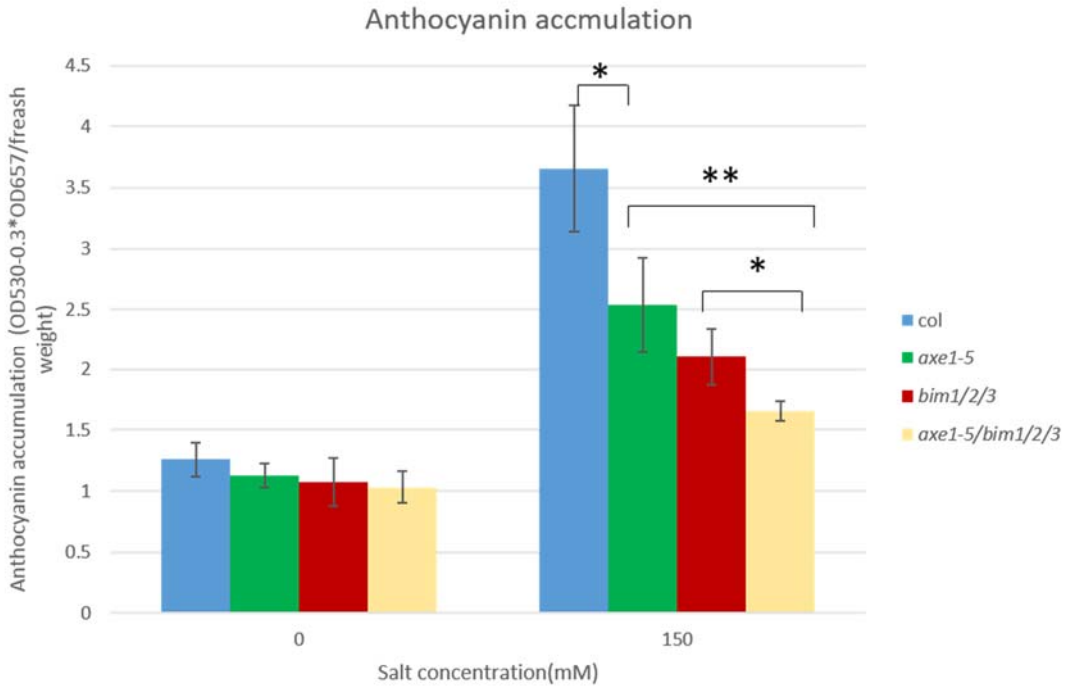

Figure 13. Anthocyanin accumulation in Col-0, *bim1/bim2/bim3*, *axe1-5* and *hda15-1* plant treated with NaCl.

(A) The anthocyanin accumulation phenotype of Col-0 and *bim1/bim2/bim3* after 150 mM salt treatment. Seeds were germinated on media supplemented with different concentration of NaCl for 3 days.

(B) The anthocyanin accumulation of *bim1/bim2/bim3*, *axe1-5* and *hda15-1* under salt stress..Seeds were germinated on 1/2MS media for 4 days and then transferred to 1/2 MS media with or without 150 mM NaCl for 14 days. Data are means ± SD of three independent biological replicates. **, P<0.01 and *, P<0.05, Student's t test.

(C) The anthocyanin accumulation of *bim1/bim2/bim3*, *axe1-5/bim1/2/3* , *axe1-5* ,

hda15-1 and Col-0. Seeds were germinated on 1/2MS media for 4 days and then transferred to 1/2 MS media with or without 150 mM NaCl for 14 days. Data are means ± SD of three independent biological replicates. **, $P<0.01$ and *, $P<0.05$, Student's t test.

Tables

Table 1. Chromatin-related proteins interacting with HDA15

AGI	Symbol	Description
Histone demethylases		
AT1G62830	LDL1	LSD1-like 1, lysine-specific histone demethylase 1 homolog 1
AT3G10390	FLD	Flowering locus D, lysine-specific histone demethylase 1 homolog 3
Histone acetyltransferases		
AT3G54610	GCN5/HAT1	General control non-repressible 5/histone acetyltransferase 1
AT1G79000	HAC1	Histone acetyltransferase of the CBP family 1
AT1G67220	HAC2	Histone acetyltransferase of the CBP family 2
AT1G55970	HAC4	Histone acetyltransferase of the CBP family 4
Histon methyltransferases		
AT2G17900	SDG37	SET domain group protein 37
AT1G02580	SDG5/MEA	SET domain group protein 5/histone-lysine N-methyltransferase MEDEA
AT4G15180	SDG2/ATXR3	SET domain group protein 2/histone-lysine N-methyltransferase ATXR3
DNA methyltransferases		
AT4G14140	DMT2	DNA methyltransferase 2
AT5G04060	PMT7	Putative methyltransferase 7
Other chromatin related proteins		
AT1G48410	AGO1	Argonaute 1
AT2G27040	AGO4	Argonaute 4
AT2G44980	CHR10	Chromatin remodeling 10
AT2G02090	CHR19	Chromatin remodeling 19
AT3G13782	NAP1;4	Nucleosome assembly protein1;4
AT5G20320	DCL4	Dicer-like protein 4
AT2G27100	SE	SERRATE, RNA effector molecule

Table 2. Transcription factors interacting with HDA15

AGI	Symbol	Description
MADS-box proteins		
AT1G01530	AGL28	Agamous-like 28
AT5G51860	AGL72	Agamous-like 72
AT3G30260	AGL79	Agamous-like 79
AT2G22540	SVP	Short vegetative phase
AT1G69120	AP1	Floral homeotic protein APETALA 1
WRKY proteins		
AT5G45050	WRKY16	WRKY transcription factor 16
AT5G24110	WRKY30	WRKY transcription factor 30
AT2G46130	WRKY43	WRKY transcription factor 43
AT5G28650	WRKY74	WRKY transcription factor 74
bHLH proteins		
AT4G00870	bHLH14	bHLH transcription factor 14
AT1G68810	bHLH30	bHLH transcription factor 30
AT5G65320	bHLH99	bHLH transcription factor 99
AT3G26744	ICE1	Inducer of CBF expression 1
AT2G43010	PIF4	Phytochrome interacting factor 4
AT4G02590	UNE12	Unfertilized embryo sac 12
MYB proteins		
AT1G22640	MYB3	MYB domain protein 3
AT2G16720	MYB7	MYB domain protein 7
AT2G39880	MYB25	MYB domain protein 25
AT5G12870	MYB46	MYB domain protein 46
AT1G18710	MYB47	MYB domain protein 47
AT5G11050	MYB64	MYB domain protein 64
AT5G49620	MYB78	MYB domain protein 78
AT2G26960	MYB81	MYB domain protein 81
AT3G49690	MYB84	MYB domain protein 84
AT5G55020	MYB120	MYB domain protein 120
AT1G09770	CDC5	Cell division cycle 5

AT1G18330	EPR1	Early-phytochrome-responsive1
AT3G04030	MYR2	MYB family transcription factor
AT3G46640	PCL1/LUX	Phytoclock 1/Lux arrhythmo
AT5G42630	ATS/KAN4	Aberrant testa shape/KANADI 4
AT1G49560		MYB family transcription factor
AT2G38300		Similar to myb family transcription factor

ARF family proteins

AT1G34170	ARF13	Auxin response factor 13
AT1G35540	ARF14	Auxin response factor 14

NAC family proteins

AT3G01600	NAC044	NAC domain containing protein 44
AT3G10490	NAC052	NAC domain containing protein 52

Zinc finger proteins

AT2G26000	BRIZ2	BRAP2 RING ZNF UBP domain-containing protein 2
AT3G17611	RBL14	Rhomboid-like protein 14
AT5G56900		Zinc finger CCCH domain-containing protein 64
AT3G20010		RING finger-related, SNF2 and helicase domain-containing protein
AT5G03450		RING finger domain-containing protein
AT2G17975		Zinc finger (Ran-binding) domain-containing protein
AT5G38600		Proline-rich spliceosome-associated family protein / zinc knuckle (CCHC-type) family protein

Other transcription factors

AT5G60120	TOE2	Target of early activation tagged (EAT) 2, AP2-like ethylene-responsive transcription factor
AT2G02540	HB21	Homeobox protein 21
AT2G12940	UNE4	Unfertilized embryo sac 4, bZIP domain protein
AT3G05690	NF-YA2	Nuclear transcription factor Y subunit A-2
AT2G33835	FES1	Frigida-essential 1, Zinc finger CCCH domain-containing protein 27

Table 3. T-DNA insertion mutants used for this study

Genes	AGI code	Mutant lines	Mutant type	Mutant site
BIM1	AT5G08130	*bim1*(SALK-85924)	T-DNA insertion	2th Exon
BIM2	AT1G69010	*bim2*(SALK-074689)	T-DNA insertion	5th Exon
BIM3	AT5G38860	*bim3*(SALK-79683)	T-DNA insertion	1st Exon
HDA6	AT5G63110	*axe1-5*(CS66153)	point mutation	G1636A
HDA15	AT3G18520	*hda15-1*(SALK-004027)	T-DNA insertion	2th Exon
		hda15-2(SALK-007520)	T-DNA insertion	3'UTR

Table 4. Primers used for T-DNA line screening

Primer name	Primer sequence
BIM1-pr1	5' CGAATTTGGTGACTTCTGCC 3'
BIM1-pr2	5' GTGACTACCTGCTTCACGTA 3'
BIM2-pr1	5' TTTGCACCCGCAAGGCTTTC 3'
BIM2-pr3	5' TGAAGGTGGTCGCTATGCTC 3'
BIM3-pr1	5' CAGATTGTTGGAGTTGGCTC 3'
BIM3-pr2	5' GGTTGGGGATTGATACCACA 3'
axe-WA-2	5' TAAGACGATGGAGGATTCACG 3'
axe-1636A-2	5' CCCAAAGATATGGAGAGGATAAGA 3'
axe-1635A-2	5' CCCAAAGATATGGAGAGGATAAAG 3'

Table 5. Primers used for plasmid constructions

Primer name	Primer sequence
BIM2-f-pr atg	5' ATGAGAACCGGAAAAGGAAA 3'
BIM2-R-stop	5' TCACAGTGTTTTCATCCGCT 3'
BIM2-r-pr rns	5' CAGTGTTTTCATCCGCTTGT 3'
BIM1-f-pr atg	5' ATGGAGCTTCCTCAACCTCGTCC 3'
BIM1-r-pr rns	5' CTGTCCCGTCTTGAGCCGTTTT 3'
BIM1-f-pr stop	5' CTACTGTCCCGTCTTGAGCCGTTT 3'
BIM3-f-pr atg	5' ATGAACTCTCATGATATCGATGATCAGTTAG 3'
BIM3-r-pr rns	5' TCGTCTTATTCTCTTCTGGGAATGATC 3'
BIM3-f-pr stop	5' TTATCGTCTTATTCTCTTCTGGGAATGATC 3'
ICE1.1-F-pr	5' ATGGGTCTTGACGGAAACAATGGTG 3'
ICE1.1-R-pr1	5' GATCATACCAGCATACCCTGCTGTATC 3'
CDC5-F-pr	5' ATGAGGATTATGATTAAGGGAGGTGTTTG 3'
CDC5-R-pr1	5' TGCAGAAGCTTCCATGGCTATG 3'
TPL-F-pr	5' ATGTCTTCTCTTAGTAGAGAGCTCGTTTTCTTG 3'
TPL-R-pr1	5' TCTCTGAGGCTGATCAGATGCAGAG 3'
MAC3B.1-F-pr	5' ATGAACTGTGCAATTTCAGGAGAAGTTC 3'
MAC3B.1-R-pr1	5' CGAGTCTTGCGCAGAGTCATCATC 3'
MOS4-F-pr	5' ATGGCGACGAACAATGGTGATG 3'
MOS4-R-pr1	5' TTGCATTTGAAGTGGCTCGACG 3'
SE-F-pr	5' ATGGCCGATGTTAATCTTCCTCCG 3'
SE-R-pr1	5' CAAGCTCCTGTAATCAATAACGGTCACTTC 3'
TIFY8-F-pr	5' ATGATGGTGAACCACAACAATGGC 3"
TIFY8-R-pr2	5' TGTGGCTTCTTTTTCAGGATCTGATCTG 3'
AGL72-F-pr	5' ATGGTGAGAGGAAAGATCGAAATCAAGAAG 3'
AGL72-R-pr1	5' TGGTCGGTTCTTCAGAAATCCAATAAATAGATC 3'
AGL79-F-pr	5' ATGGGAAGAGGAAGGGTTCAGCTAC 3'
AGL79-R-pr1	5' TTCTCCGGTGAGCTGGGGCATC 3'
bHLH99-F-pr	5' ATGATGTTCCAACAAGATTACCCTCATG 3'
bHLH99-R-pr1	5' ACGTTCCTTGTGAACTCTTCTAACGACTTC 3'

Supplementary Tables

Supplementary Table 1. Additional proteins interacting with HDA15

AGI	Symbol	Description
Regulation of transcription		
AT1G24190	SNL3	SIN3-like 3
AT1G70060	SNL4	SIN3-like 4
AT2G45640	SAP18	SIN3 associated polypeptide P18
AT3G04580	EIN4	Ethylene insensitive 4
AT2G02470	AL6	Alfin-like 6
AT3G47610		Transcription regulator/ zinc ion binding protein
Hormone		
AT1G75310	AUL1	Auxin-like 1 protein
AT5G65980	PILS7	PIN-likes 7
AT2G46690	SAUR32	Small auxin upregulated RNA 32
AT4G31320	SAUR37	Small auxin upregulated RNA 37
AT1G78440	GA2ox1	Gibberellin 2-beta-dioxygenase 1
AT4G19170	NCED4	Nine-cis-epoxycarotenoid dioxygenase 4
AT3G13380	BRL3	BRI1-like 3, similar to BRI, brassinosteroid receptor protein
Response to abiotic stimulus		
AT1G62380	ACO2	ACC oxidase 2, 1-aminocyclopropane-1-carboxylate oxidase 2
AT1G73330	DR4	Drought-repressed 4
AT4G27430	CIP7	COP1-interacting protein 7
AT5G61150	VIP4	Vernalization independence 4
AT4G13850	GR-RBP2	Glycine-rich RNA-binding protein 2
AT4G39260	CCR1/GR-RBP8	Cold, circadian rhythm, and RNA binding 1/Glycine-rich RNA-binding protein 8
AT3G52800	SAP6	Zinc finger A20 and AN1 domain-containing stress-associated protein 6
AT3G56240	CCH	Copper chaperone
AT3G19820	DWF1	DWARF 1, Ca2+-dependent calmodulin-binding protein

Response to light stimulus

AT1G09570	PHYA	Phytochrome A
AT5G35840	PHYC	Phytochrome C
AT5G24850	CRY3	Cryptochrome 3
AT3G47470	LHCA4	Chlorophyll a-b binding protein 4
AT5G04190	PKS4	Phytochrome kinase substrate 4

Ubiquitin-protein ligase activity

AT3G50080	VFB2	VIER F-box protein 2
AT4G07400	VFB3	VIER F-box proteine 3
AT2G32950	COP1	Constitutive photomorphogenic 1, E3 ubiquitin-protein ligase
AT5G62800	SINA-like 11	E3 ubiquitin-protein ligase
AT2G33340	MAC3B	MOS4-associated complex 3B, U-box protein
AT5G15400	MUSE3	Mutant, SNC1-enhancing 3, probable ubiquitin conjugation factor E4
AT5G27420	ATL31	Arabidopsis toxicos en levadura 31, E3 ubiquitin-protein ligase
AT1G57800	VIM5	Variant in methylation 5, E3 ubiquitin-protein ligase
AT1G55250	HUB2	Histone mono-ubiquitination 2, E3 ubiquitin-protein ligase
AT5G63730	ARI14	ARIADNE 14, E3 ubiquitin-protein ligase
AT1G03365	RF4	E3 ubiquitin-protein ligase
AT4G08940		Ubiquitin carboxyl-terminal hydrolase family protein

Protein kinase activity

AT3G07980	MAPKKK6	Mitogen-activated protein kinase kinase kinase 6
AT1G01560	MAPK11	Mitogen-activated protein kinase 11
AT2G42880	MAPK20	Mitogen-activated protein kinase 20
AT3G16030	CES101	Callus expression of RBCS 101, G-type lectin S-receptor-like serine/threonine-protein kinase
AT3G25840	PRP4	Serine/threonine-protein kinase
AT5G64960	CDKC2	Cyclin-dependent kinase C-2
AT5G41990	WNK8	Serine/threonine-protein kinase
AT1G65800	RK2	Receptor kinase 2, receptor-like serine/threonine-protein kinase SD1-6
AT1G16760		Protein kinase protein with adenine nucleotide alpha hydrolases-like domain

AT2G41930		Protein serine/threonine kinase
AT3G09830		Protein kinase family protein

WD40/YVTN repeat-like

AT1G80490	TPR1	Topless-related protein 1
AT5G27640	TIF3B1	Translation initiation factor 3 subunit B
AT2G37670		WD-40 repeat-containing protein
AT5G19920		WD40 domain-containing protein
AT3G50590		Transducin/WD40 domain-containing protein

Seed development

AT4G27150	SESA2	Seed storage albumin 2
AT4G27160	SESA3	Seed storage albumin 3
AT5G23940	PEL3	Permeable leaves3, acyl-transferase
AT2G42560		Late embryogenesis abundant domain-containing protein
AT3G17520		Late embryogenesis abundant protein (LEA) family protein
AT2G10940		Bifunctional inhibitor/lipid-transfer protein/seed storage 2S albumin superfamily protein

DNA/RNA-binding

AT5G53060	RCF3	Regulator of CBF gene expression 3, RNA-binding protein
AT5G51120	PABN1	Polyadenylate-binding protein 1
AT2G34160		Alba DNA/RNA-binding protein
AT1G27750		Nucleic acid binding protein
AT1G51530		RNA-binding (RRM/RBD/RNP motifs) family protein

Peroxidase activity

AT5G51060	RHD2/RBOHC	Root hair defective 2/Respiratory burst oxidase homolog protein C
AT1G05240		Peroxidase 1
AT1G71695		Peroxidase 12
AT3G49960		Peroxidase 35
AT4G26010		Peroxidase 44
AT5G17820		Peroxidase 57
AT5G64100		Peroxidase 69

Ribosome

AT5G57020	NMT1	N-myristoyltransferase 1
AT2G04390		40S ribosomal protein S17-1
AT5G02960		40S ribosomal protein S23-2
AT3G04920		40S ribosomal protein S24-1
AT5G28060		40S ribosomal protein S24-2
AT4G34670		40S ribosomal protein S3a-2
AT2G37270		40S ribosomal protein S5-1
AT2G42740	RPL16A	60S ribosomal protein L16A
AT3G53020	RPL24B	60S ribosomal protein L24-2
AT3G60245		60S ribosomal protein L37a-2
AT2G43460		60S ribosomal protein L38
AT3G10950		60S ribosomal protein L37a-1
AT1G01100		60S acidic ribosomal protein P1-1

Ion binding

AT1G50560	CYP705A25	Cytochrome P450, family 705, subfamily A, polypeptide 25
AT3G26130		Cellulase (glycosyl hydrolase family 5) protein
AT5G53460	GLT1	NADH-dependent glutamate synthase 1
AT5G64210	AOX2	Alternative oxidase 2
AT4G36390		Methylthiotransferase
AT1G08130	LIG1	DNA ligase 1
AT4G27800	TAP38/PPH1	Protein phosphatase
AT3G44340	CEF	Clone eighty-four, transport protein Sec24-like
AT5G17980		C2 calcium/lipid-binding and phosphoribosyltransferase C-terminal domain-containing protein

Other

AT4G32570	TIFY8	TIFY domain protein 8
AT1G30480	DRT111	DNA-damage-repair/toleration protein 111
AT1G55310	SR33	SC35-like splicing factor 33
AT3G57150	NAP57	Pseudouridine synthase
AT5G62190	PRH75	DEAD/DEAH box RNA helicase
AT1G18730	NDF6	NDH dependent flow 6
AT1G80070	SUS2	Abnormal suspensor 2
AT1G16610	SR45	Arginine/serine-rich 45

AT1G63680	MURE	UDP-N-acetylmuamoylalanyl-d-glutamate-2,6-diaminopimelate ligase
AT5G44270	TPX2	Targeting protein for Xklp2
AT5G55310	TOP1	Topoisomerase 1
AT5G14060	CARAB-AK-LYS	Lysine-sensitive aspartate kinase
AT2G36420	TRM27	TON1 recruiting motif 27
AT2G34700		Pollen Ole e 1 allergen and extensin family protein
AT5G19760		Mitochondrial substrate carrier family protein
AT2G29210		Splicing factor PWI domain-containing protein
AT1G21780		BTB/POZ domain-containing protein
AT3G06340		DnaJ domain-containing protein
AT2G05580		Glycine-rich protein
AT1G24300		GYF domain-containing protein
AT4G14490		SMAD/FHA domain-containing protein
AT1G47540		Defensin-like protein 192
AT2G22610		Di-glucose binding protein with Kinesin motor domain
AT1G62130		AAA-type ATPase-like protein
AT3G01520		Adenine nucleotide alpha hydrolases-like superfamily protein
AT1G13310		Endosomal targeting BRO1-like domain-containing protein
AT4G32620		Enhancer of polycomb-like transcription factor protein
AT5G20950		Glycosyl hydrolase family protein
AT1G78910		RNA pseudourine synthase 3
AT2G22720		SPT2 chromatin protein
AT2G22880		VQ motif-containing protein
AT1G11900		Tetratricopeptide repeat (TPR)-like superfamily protein
AT4G16960		Disease resistance protein (TIR-NBS-LRR class) family
AT3G48810		Pentatricopeptide repeat (PPR) superfamily protein
AT5G40400		Pentatricopeptide repeat (PPR) superfamily protein
AT5G26290		TRAF-like family protein
AT5G26280		TRAF-like family protein
AT2G04170		TRAF-like family protein
AT5G26260		TRAF-like family protein
AT2G04190		TRAF-like family protein
AT5G53440		Hypothetical protein
AT1G08580		Hypothetical protein

AT4G15640	Hypothetical protein
AT5G13260	Hypothetical protein
AT5G14990	Hypothetical protein
AT1G20520	Hypothetical protein
AT5G45660	Hypothetical protein
AT2G45840	Hypothetical protein
AT5G24350	Hypothetical protein
AT5G55520	Hypothetical protein
AT5G56060	Hypothetical protein
AT5G57370	Hypothetical protein
AT5G22040	Hypothetical protein
AT4G19370	Hypothetical protein
AT5G19950	Hypothetical protein
AT5G38720	Hypothetical protein
AT3G52900	Hypothetical protein

References

Ahringer, J. (2000). NuRD and SIN3: histone deacetylase complexes in development. Trends Genet. **16:**351-356.

Alinsug, M.V., Chen, F.F., Luo, M., Tai, R., Jiang, L., and Wu, K. (2012). Subcellular localization of class II HDAs in Arabidopsis thaliana: nucleocytoplasmic shuttling of HDA15 is driven by light.PLoS One **7:**e30846-e30846.

Baba, A., Ohtake, F., Okuno, Y., Yokota, K., Okada, M., Imai, Y., Ni, M., Meyer, C.A., Igarashi, K., and Kanno, J. (2011). PKA-dependent regulation of the histone lysine demethylase complex PHF2-ARID5B. Nat. Cell Biol. **13:**668-675.

Barbero, J.L. (2009). Cohesins: chromatin architects in chromosome segregation, control of gene expression and much more. Cell. Mol. Life Sci. **66:**2025-2035.

Bate, N.J., and Rothstein, S.J. (1998). C6-volatiles derived from the lipoxygenase pathway induce a subset of defense-related genes. Plant J. **16:**561-569.

Belkhadir, Y., and Jaillais, Y. (2015). The molecular circuitry of brassinosteroid signaling. New Phytol.**206:**522-540.

Chen, L.-T., Luo, M., Wang, Y.-Y., and Wu, K. (2010). Involvement of Arabidopsis histone deacetylase HDA6 in ABA and salt stress response. J. Exp. Bot.

61:3345-3353.

Chini, C.C., Escande, C., Nin, V., and Chini, E.N. (2010). HDAC3 is negatively regulated by the nuclear protein DBC1. J. Biol. Chem. **285:**40830-40837.

Chinnusamy, V., Ohta, M., Kanrar, S., Lee, B.-h., Hong, X., Agarwal, M., and Zhu, J.-K. (2003). ICE1: a regulator of cold-induced transcriptome and freezing tolerance in Arabidopsis. Genes Dev. **17:**1043-1054.

Choudhary, S.P., Yu, J.-Q., Yamaguchi-Shinozaki, K., Shinozaki, K., and Tran, L.-S.P. (2012). Benefits of brassinosteroid crosstalk. Trends Plant Sci. **17:**594-605.

Fuchs, J., Demidov, D., Houben, A., and Schubert, I. (2006). Chromosomal histone modification patterns–from conservation to diversity. Trends Plant Sci. **11:**199-208.

Guan, Q., Wen, C., Zeng, H., and Zhu, J. (2013). A KH domain-containing putative RNA-binding protein is critical for heat stress-responsive gene regulation and thermotolerance in Arabidopsis. Mol. Plant. **6:**386-395.

Guo, H., Li, L., Aluru, M., Aluru, S., and Yin, Y. (2013). Mechanisms and networks for brassinosteroid regulated gene expression. Curr. Opin. Plant Biol. **16:**545-553.

Han, Z., Guo, L., Wang, H., Shen, Y., Deng, X.W., and Chai, J. (2006). Structural basis for the specific recognition of methylated histone H3 lysine 4 by the WD-

40 protein WDR5. Mol. Cell **22:**137-144.

Henikoff, S. (2005). Histone modifications: combinatorial complexity or cumulative simplicity? Proc. Natl. Acad. Sci. U. S. A. **102:**5308-5309.

Jones, J.D., and Dangl, J.L. (2006). The plant immune system. Nature **444:**323-329.

Joshi, P., Guise, A.J., Luo, Y., Yu, F., Nesvizhskii, A.I., Cristea, I.M. (2013). The functional interactome landscape of the human histone deacetylase family. Mol Syst Biol. **9**:672.

Kim, J.-E., Chen, J., and Lou, Z. (2008). DBC1 is a negative regulator of SIRT1. Nature **451:**583-586.

Li, J. (2005). Brassinosteroid signaling: from receptor kinases to transcription factors. Curr. Opin. Plant Biol. **8:**526-531.

Li, J., and Jin, H. (2007). Regulation of brassinosteroid signaling. Trends Plant Sci. **12:**37-41.

Li, X., Clarke, J.D., Zhang, Y., and Dong, X. (2001). Activation of an EDS1-mediated R-gene pathway in the snc1 mutant leads to constitutive, NPR1-independent pathogen resistance. Mol. Plant-Microbe Interact. **14:**1131-1139.

Liu, X., Chen, C.-Y., Wang, K.-C., Luo, M., Tai, R., Yuan, L., Zhao, M., Yang, S., Tian, G., and Cui, Y. (2013). PHYTOCHROME INTERACTING FACTOR3 associates with the histone deacetylase HDA15 in repression of chlorophyll

biosynthesis and photosynthesis in etiolated Arabidopsis seedlings. Plant Cell **25:**1258-1273.

Luo, M., Wang, Y.-Y., Liu, X., Yang, S., Lu, Q., Cui, Y., and Wu, K. (2012). HD2C interacts with HDA6 and is involved in ABA and salt stress response in Arabidopsis. J. Exp. Bot. **63:**3297-3306.

Müssig, C., Biesgen, C., Lisso, J., Uwer, U., Weiler, E.W., and Altmann, T. (2000). A novel stress-inducible 12-oxophytodienoate reductase from Arabidopsis thaliana provides a potential link between brassinosteroid-action and jasmonic-acid synthesis. J. Plant Physiol.**157:**143-152.

Mitchell, J., Mandava, N., Worley, J., Plimmer, J., and Smith, M. (1970). Brassins-a new family of plant hormones from rape pollen. Nature **225:**1065-1066.

Monaghan, J., Xu, F., Gao, M., Zhao, Q., Palma, K., Long, C., Chen, S., Zhang, Y., and Li, X. (2009). Two Prp19-like U-box proteins in the MOS4-associated complex play redundant roles in plant innate immunity. PLoS Pathog. **5:**e1000526-e1000526.

Oh, E., Zhu, J.-Y., Ryu, H., Hwang, I., and Wang, Z.-Y. (2014). TOPLESS mediates brassinosteroid-induced transcriptional repression through interaction with BZR1. Nat. Commun. **5:**4140.

Palma, K., Zhao, Q., Cheng, Y.T., Bi, D., Monaghan, J., Cheng, W., Zhang, Y., and

Li, X. (2007). Regulation of plant innate immunity by three proteins in a complex conserved across the plant and animal kingdoms. Genes Dev. **21:**1484-1493.

Pandey, R., MuÈller, A., Napoli, C.A., Selinger, D.A., Pikaard, C.S., Richards, E.J., Bender, J., Mount, D.W., and Jorgensen, R.A. (2002). Analysis of histone acetyltransferase and histone deacetylase families of Arabidopsis thaliana suggests functional diversification of chromatin modification among multicellular eukaryotes. Nucleic Acids Res. **30:**5036-5055.

Peng, Z., Han, C., Yuan, L., Zhang, K., Huang, H., and Ren, C. (2011). Brassinosteroid enhances jasmonate - induced anthocyanin accumulation in Arabidopsis seedlings. Journal of integrative plant biology **53:**632-640.

Schaller, F., Biesgen, C., Müssig, C., Altmann, T., and Weiler, E.W. (2000). 12-Oxophytodienoate reductase 3 (OPR3) is the isoenzyme involved in jasmonate biosynthesis. Planta **210:**979-984.

Shahbazian, M.D., and Grunstein, M. (2007). Functions of site-specific histone acetylation and deacetylation. Annu. Rev. Biochem. **76:**75-100.

Shinozaki, K., and Yamaguchi-Shinozaki, K. (2007). Gene networks involved in drought stress response and tolerance. J. Exp. Bot. **58:**221-227.

Song, C.-P., and Galbraith, D.W. (2006). AtSAP18, an orthologue of human SAP18,

is involved in the regulation of salt stress and mediates transcriptional repression in Arabidopsis. Plant Mol.Biol. **60:**241-257.

Vermeulen, M., Eberl, H.C., Matarese, F., Marks, H., Denissov, S., Butter, F., Lee, K.K., Olsen, J.V., Hyman, A.A., and Stunnenberg, H.G. (2010). Quantitative interaction proteomics and genome-wide profiling of epigenetic histone marks and their readers. Cell **142:**967-980.

Wang, L., Kim, J., and Somers, D.E. (2013). Transcriptional corepressor TOPLESS complexes with pseudoresponse regulator proteins and histone deacetylases to regulate circadian transcription. Proc. Natl. Acad. Sci. U. S. A. **110:**761-766.

Woloshen, V., Huang, S., and Li, X. (2010). RNA-Binding Proteins in Plant Immunity. J. Pathog. **2011:**278697-278697.

Xie, Z., Allen, E., Wilken, A., and Carrington, J.C. (2005). DICER-LIKE 4 functions in trans-acting small interfering RNA biogenesis and vegetative phase change in Arabidopsis thaliana. Proc. Natl. Acad. Sci. U. S. A. of the United States of America **102:**12984-12989.

Yin, Y., Vafeados, D., Tao, Y., Yoshida, S., Asami, T., and Chory, J. (2005). A new class of transcription factors mediates brassinosteroid-regulated gene expression in Arabidopsis. Cell **120:**249-259.

Yu, C.-W., Liu, X., Luo, M., Chen, C., Lin, X., Tian, G., Lu, Q., Cui, Y., and Wu,

K. (2011). HISTONE DEACETYLASE6 interacts with FLOWERING LOCUS D and regulates flowering in Arabidopsis. Plant Physiol. **156:**173-184.

Zhang, Y., Goritschnig, S., Dong, X., and Li, X. (2003). A gain-of-function mutation in a plant disease resistance gene leads to constitutive activation of downstream signal transduction pathways in suppressor of npr1-1, constitutive 1. Plant Cell **15:**2636-2646.

Zhao, W., Kruse, J.-P., Tang, Y., Jung, S.Y., Qin, J., and Gu, W. (2008). Negative regulation of the deacetylase SIRT1 by DBC1. Nature **451:**587-590.

Zhu, J.-K. (2001). Plant salt tolerance. Trends Plant Sci. **6:**66-71.

Zimmerli, L., Métraux, J.-P., and Mauch-Mani, B. (2001). β-Aminobutyric acid-induced protection of Arabidopsis against the necrotrophic fungus Botrytis cinerea. Plant Physiol. **126:**517-523.